NASA SP-126

SURVEYOR I

A Preliminary Report

NATIONAL AERONAUTICS AND SPACE ADMINISTRATION

NASA SP-126

SURVEYOR I

A Preliminary Report

Compiled by
Lunar and Planetary Programs Division
Office of Space Science and Applications

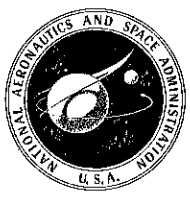

Scientific and Technical Information Division JUNE 1966
NATIONAL AERONAUTICS AND SPACE ADMINISTRATION
Washington, D.C.

FOREWORD

IN THE DIFFICULT AND CHANCY EXPLORATION OF SPACE, it is rare that a first mission flown by an unmanned spacecraft achieves all its objectives – and more. The brilliantly successful flight of Surveyor I was all the more notable because it incorporated many operationally new elements. Among these were the Centaur high-energy, hydrogen-fueled rocket serving as the second stage of the launch vehicle, three throttleable vernier rockets, extremely sensitive velocity- and altitude-sensing radars, and an automatic closed-loop guidance and control system that, in the terminal phase of the flight, precisely steered and decelerated the spacecraft to a soft landing. Finally, there was the survey television that – at this writing – has already sent back more than 10 000 pictures of high scientific content.

That these and scores of other complex subsystems performed almost exactly as designed is testimony to the skill, imagination, and dedication of the thousands of people who brought about this extraordinary achievement. It is also testimony, in a broader sense, to the Nation's steadily mounting proficiency in the design, testing, and flight of space vehicles.

This publication, preliminary in nature, has been compiled even before the full functioning "lifetime" of Surveyor I has been established. It does not attempt to present detailed measurement and analysis of the immense amounts of scientific data that the spacecraft has telemetered to Earth; this task will take months and even years. But in the interest of quickly reporting the scientific interpretations made during the first days in the "life" of Surveyor I, the National Aeronautics and Space Administration has compiled this initial report on that spacecraft's remarkable achievements.

HOMER E. NEWELL, *Associate Administrator for Space Science and Applications*
National Aeronautics and Space Administration

June 17, 1966

SUMMARY

THE SURVEYOR I SPACECRAFT *was launched on May 30, 1966, from Cape Kennedy, Florida, on a direct-ascent lunar trajectory. Approximately 16 hours after launch, a successful midcourse correction maneuver was executed, moving the landing point some 35 miles to an area north of the crater Flamsteed in Oceanus Procellarum. Because telemetry indicated that one of the two omnidirectional antennas may not have fully deployed, a terminal maneuver was used which assured correct Earthward orientation of the deployed antenna during descent. The spacecraft properly executed all commands, and the automatic closed-loop descent sequence was completed at 06 17 36 GMT on June 2, 1966. Preliminary data reduction indicates that the spacecraft touched down at a vertical velocity of approximately 10 fps at 2.41° S. lat. and 43.34° W long.*

During its first five days of operation on the Moon, Surveyor I transmitted more than 4000 pictures. Following are the preliminary findings by the Surveyor Scientific Evaluation and Analysis Team and associated working groups on the scientific data received up to that time:

Surveyor I landed on a dark, relatively smooth, bare surface, encircled by hills and low mountains. The crestlines of a few of these low mountains are visible along the horizon, from which the spacecraft may be located accurately with respect to the major features of the lunar surface. Observations of Sirius and Canopus and numerous points on the horizon show that the landing site is smooth and nearly level on a kilometer scale.

The terrain within 1 to 2 km surrounding the Surveyor I landing site is a gently rolling surface studded with craters with diameters from a few centimeters to several hundred meters and littered with fragmental debris ranging in size from less than 1 mm to more than 1 m. The larger craters observed resemble those seen in the Ranger photographs in shape and distribution. Thus the Surveyor I landing site appears to be a representative sample of a mare surface.

The surface is composed of granular material of a wide size range; coarse blocks of rock and smaller fragments are set in a matrix of fine particles too small to be resolved. This material was disturbed and penetrated by the footpads of the spacecraft to a depth of a few centimeters. The shapes of small craters suggest that the fragmental layer may extend to depths of at least a meter.

The material disturbed by the spacecraft footpads is made up of lumps that are probably aggregates of much finer grains, 1 mm or less in diameter. These aggregates show that the fragmental material on the local lunar surface is at least slightly cohesive. Some disturbed material was thrown out to form rays, similar in shape and apparent genesis to those observed from Earth around some large craters, but darker than the adjacent surface.

If the material is homogeneous to a depth of some tens of centimeters, the soil appears to have a static bearing capacity, on this scale, of about 5 psi (3×10^5 dynes/cm^2).

Thermal data, as shown by a comparison of predicted and actual spacecraft temperatures, indicate that the spacecraft temperature-control surfaces are not covered by dust.

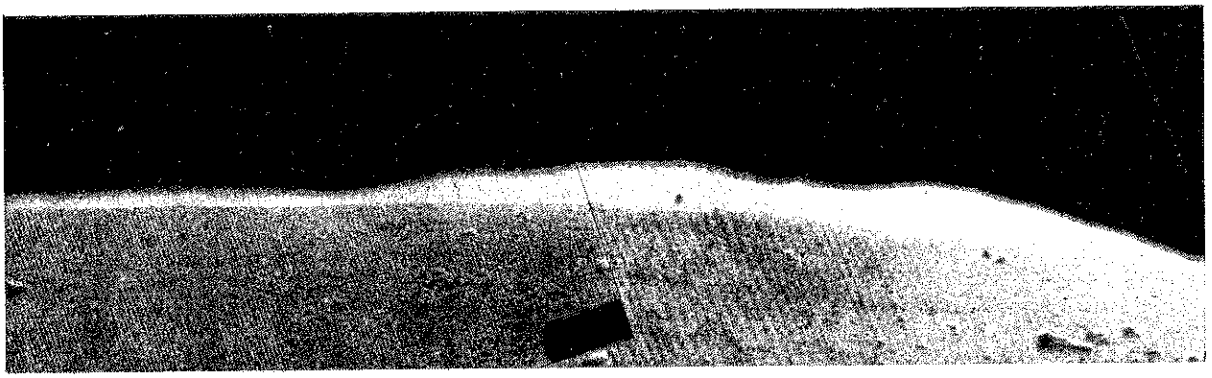

". . . a bare surface, encircled by hills and low mountains."

SURVEYOR I *A Preliminary Report*

INTRODUCTION

IN UNMANNED LUNAR EXPLORATION, the National Aeronautics and Space Administration is currently conducting two programs, Surveyor and Lunar Orbiter. The latter is planned to provide medium- and high-resolution photographs over broad areas to aid in site selection for the Apollo manned-landing program. The Surveyor program has three major objectives. One is to validate several critical aspects of advanced soft-landing techniques for later use by Apollo. Another is to provide essential data on the compatibility of the Apollo design with conditions encountered on the lunar surface. A third is to add to scientific knowledge about the Moon.

The first Surveyors have been planned to prove the design of the spacecraft, develop the critical soft-landing technique, and to acquire lunar-surface information needed for later Surveyor and Apollo missions. Subsequent spacecraft in the series will, in addition, conduct operations calculated to supply additional scientific information about the Moon and the environment at its surface.

Surveyor I, the spacecraft described here, was the first engineering test model to be flown. Though it did not carry scientific experiments, it was fitted with a survey television system and with instrumentation intended to measure bearing strength, temperatures, and radar reflectivity of the lunar surface.

The Surveyor program is being conducted under the direction of NASA's Office of Space Science and Applications, with the Jet Propulsion Laboratory providing project management. The Hughes Aircraft Company has responsibility for the design and fabrication of the spacecraft.

Prior Scientific Data

The first pictures of the Moon taken from a spacecraft were obtained at extremely long range by the Russian Luna III on October 3, 1959. The first medium- and high-resolution spacecraft pictures of the Moon were taken by Ranger VII (July 31, 1964), Ranger VIII (February 20, 1965), and Ranger IX (March 24, 1965). Collectively, these three Rangers transmitted more than 17 000 pictures having varying resolution

down to almost 1 foot. Prior to Surveyor I, the pictures of the lunar surface having the best resolution were obtained on February 3, 1966, by Luna IX, showing details of the surface down to fractions of an inch in the immediate vicinity of the landed capsule. Luna IX was reported to weigh 3480 pounds (1578 kg) at separation from the launch vehicle, and the landing capsule was said to weigh 220 pounds (100 kg). Surveyor I weighed 2194 pounds (995 kg) at separation and 596 pounds (270 kg) at landing.

Luna IX provided photographs showing the surface texture at one location on the Moon. Some inferences as to the load-bearing quality of the surface may be derived from the fact that the capsule did not sink below the surface. A number of important Surveyor I mission objectives, however, were not met by the much simpler Luna IX. These include:

- Verification of advanced closed-loop soft-landing techniques similar to those that will be used to land men on the Moon;
- Quantitative data on surface bearing strength;
- Quantitative data on radar reflectivity;
- Quantitative data on lunar-surface temperature ranges; and
- A determination as to whether or not there is loose dust on the Moon.

Surveyor I Mission Objectives

Detailed planning goals for this flight were established as follows:

Primary Objectives

- Demonstrate the capability of the Surveyor spacecraft to perform successful midcourse and terminal maneuvers, and to achieve a soft landing on the Moon;
- Demonstrate the capability of the Surveyor communications system and Deep Space Network to maintain communications with the spacecraft during its flight and after a soft landing; and
- Demonstrate the capability of the Atlas/Centaur launch vehicle to inject the Surveyor spacecraft on a lunar-intercept trajectory.

Secondary Objectives

- Obtain in-flight engineering data on all spacecraft subsystems used in cruise flight;
- Obtain in-flight engineering data on all subsystems used during the midcourse maneuver;
- Obtain in-flight engineering data on the performance of the closed-loop terminal descent guidance and control system, including the velocity and altitude radars, the on-board analog computer, the autopilot, and the vernier engines; and
- Obtain engineering data on the performance of subsystems used on the lunar surface.

Tertiary Objectives

- Obtain postlanding TV pictures of a spacecraft footpad and the surface material immediately surrounding it;
- Obtain postlanding TV pictures of the lunar topography;
- Obtain data on the radar reflectivity of the lunar surface;
- Obtain data on the bearing strength of the lunar surface; and
- Obtain temperature data of the spacecraft on the lunar surface, for use in analysis of lunar-surface temperatures.

VEHICLE DESCRIPTION

THE SPACE VEHICLE FOR THIS MISSION consisted of an Atlas-Centaur launch vehicle, Surveyor spacecraft, adapters between the launch-vehicle stages and between the Centaur and the spacecraft, and a clamshell-shaped fairing that enclosed the spacecraft during atmospheric flight. Figure 1 shows the vehicle during launch from Complex 36-A at Cape Kennedy.

Launch Vehicle

The Atlas-Centaur AC-10, the launch vehicle for Surveyor I, was a two-stage vehicle; the Atlas first stage was powered by the standard MA-5 propulsion system having two booster engines and a sustainer engine; the Centaur second stage was powered by two high-energy RL-10 engines, each with 15 000 pounds of thrust. The performance characteristics and dimensions of the launch vehicle are shown in figure 2.

The RL-10 engine is the first engine to operate successfully in space using liquid hydrogen as a fuel (liquid oxygen is used as the oxidizer). The Centaur was surrounded by four thermal insulation panels to minimize the boil-off of hydrogen, which was maintained at a temperature of −423° F. The panels were jettisoned after the vehicle left the atmosphere.

The nose fairing, constructed of honeycomb fiber glass, enclosed the spacecraft and guidance and electronics equipment mounted on the Centaur. The fairing provided thermal and aerodynamic protection during flight through the atmosphere and was jettisoned shortly after the insulation panels. In addition to the primary propulsion system, the Centaur was equipped with small hydrogen peroxide attitude-control thrusters and four 50-pound (222-newton) hydrogen peroxide thrusters. The larger thrusters were used during the retromaneuver that was performed after the second stage separated from the spacecraft. This maneuver altered the Centaur's trajectory sufficiently to keep the Surveyor's star sensor from mistaking the second stage for Canopus, and also to keep the Centaur from impacting the Moon.

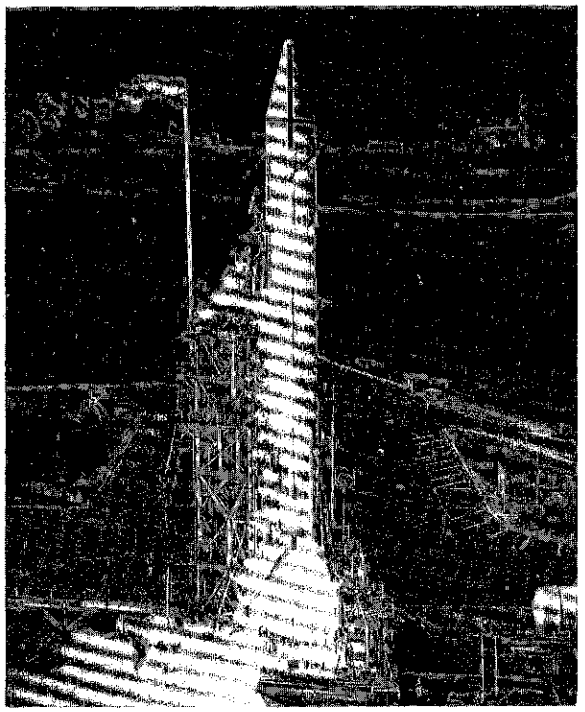

FIGURE 1. — The Atlas/Centaur launch vehicle lifts Surveyor I from Complex 36-A at Cape Kennedy, Florida, on May 30, 1966.

Spacecraft

The configuration of the Surveyor spacecraft is shown in figure 3. The basic structure, which provides mounting surfaces and attachments for the power, communications, propulsion, and flight control systems, as well as a platform for the payload packages, is constructed of thin-walled aluminum tubing with the members interconnected to form a triangle. A shock-absorbing landing leg is attached by a hinge to each of the three lower corners of the structure. The legs

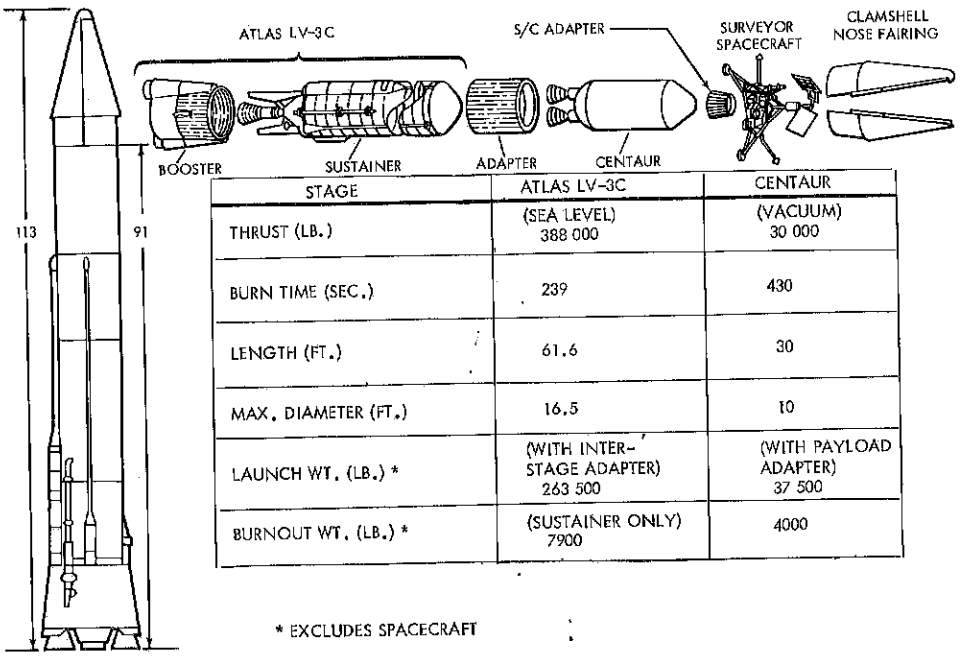

STAGE	ATLAS LV-3C	CENTAUR
THRUST (LB.)	(SEA LEVEL) 388 000	(VACUUM) 30 000
BURN TIME (SEC.)	239	430
LENGTH (FT.)	61.6	30
MAX. DIAMETER (FT.)	16.5	10
LAUNCH WT. (LB.) *	(WITH INTER-STAGE ADAPTER) 263 500	(WITH PAYLOAD ADAPTER) 37 500
BURNOUT WT. (LB.) *	(SUSTAINER ONLY) 7900	4000

* EXCLUDES SPACECRAFT

FIGURE 2. — Characteristics of the launch vehicle used for Surveyor I.

were folded into the nose fairing during launch. As additional protection against landing loads, blocks of crushable aluminum honeycomb are placed on the bottom of each corner of the frame. A vertical mast with mechanisms that position the high-gain planar array antenna and solar panel is mounted on top of the structure. The basic frame weighs less than 60 pounds (27 kg) and the installation hardware weighs 23 pounds (10 kg).

The spacecraft is some 10 feet (3 m) high, and its tripod landing gear fits just within a 14-foot (4-m) circle. Weighing 2194 pounds (995 kg) at launch, Surveyor I had a landing weight of 596 pounds (270 kg), after depletion of propellants and other consumables and after jettison of the altitude-marking radar and the main retrorocket casing.

Two thermally controlled compartments, their temperatures held within acceptable limits by a careful arrangement of absorptive and reflective paints, by conductive heat paths and thermal switches, and, on the dark side, by small electric heaters, are provided aboard the spacecraft. One compartment, held between 40° F. and 125° F., houses communications and most power-supply electronics. The other, held between 0° F. and 125° F., houses the command and signal processing functions. The solar panel, consisting of a series-parallel array of 792 solar-cell modules approximating 9 square feet in area, supplied up to 85 watts of power during cruise and on the lunar surface. Rechargeable silver-zinc batteries are used for energy storage and to accommodate peak loads. A power-management system aboard has the function of converting, regulating, and switching power as required by various subsystems.

Inertial references for detecting and controlling the attitude of the spacecraft during cruise flight, as well as during midcourse and terminal maneuvers, were provided by a Canopus star tracker, a Sun sensor, and rate gyros on three axes. During cruise flight attitude control was exercised by a subsystem employing small cold-gas thrusters. Control during terminal descent was exercised initially by the autopilot, vernier engines, and by an altitude-marking radar that began the firing of the main retrorocket. Subsequently the spacecraft was steered and decelerated by velocity-measuring and altimeter radars that, in conjunction with the on-board analog

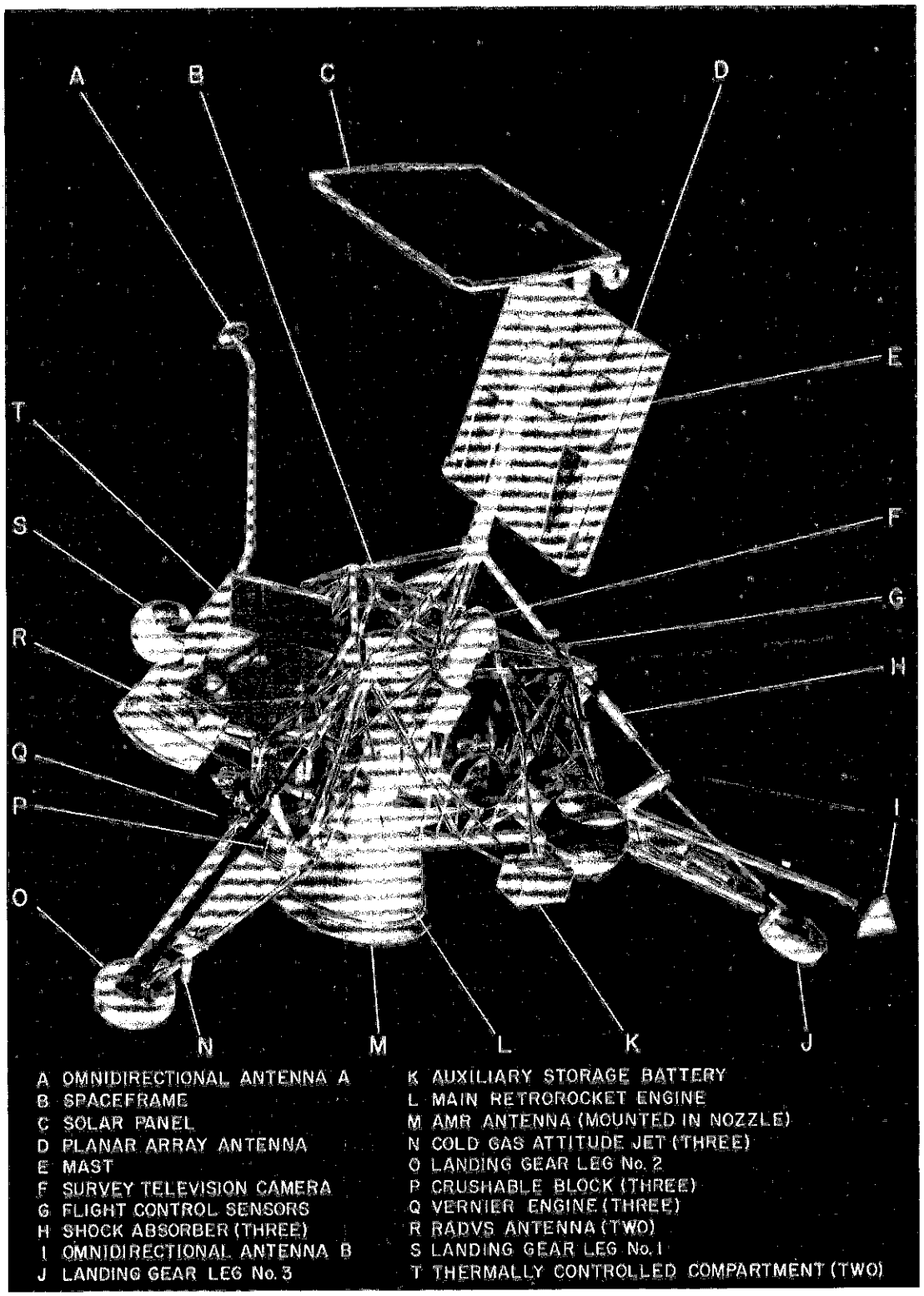

FIGURE 3. – Major components of the Surveyor I spacecraft.

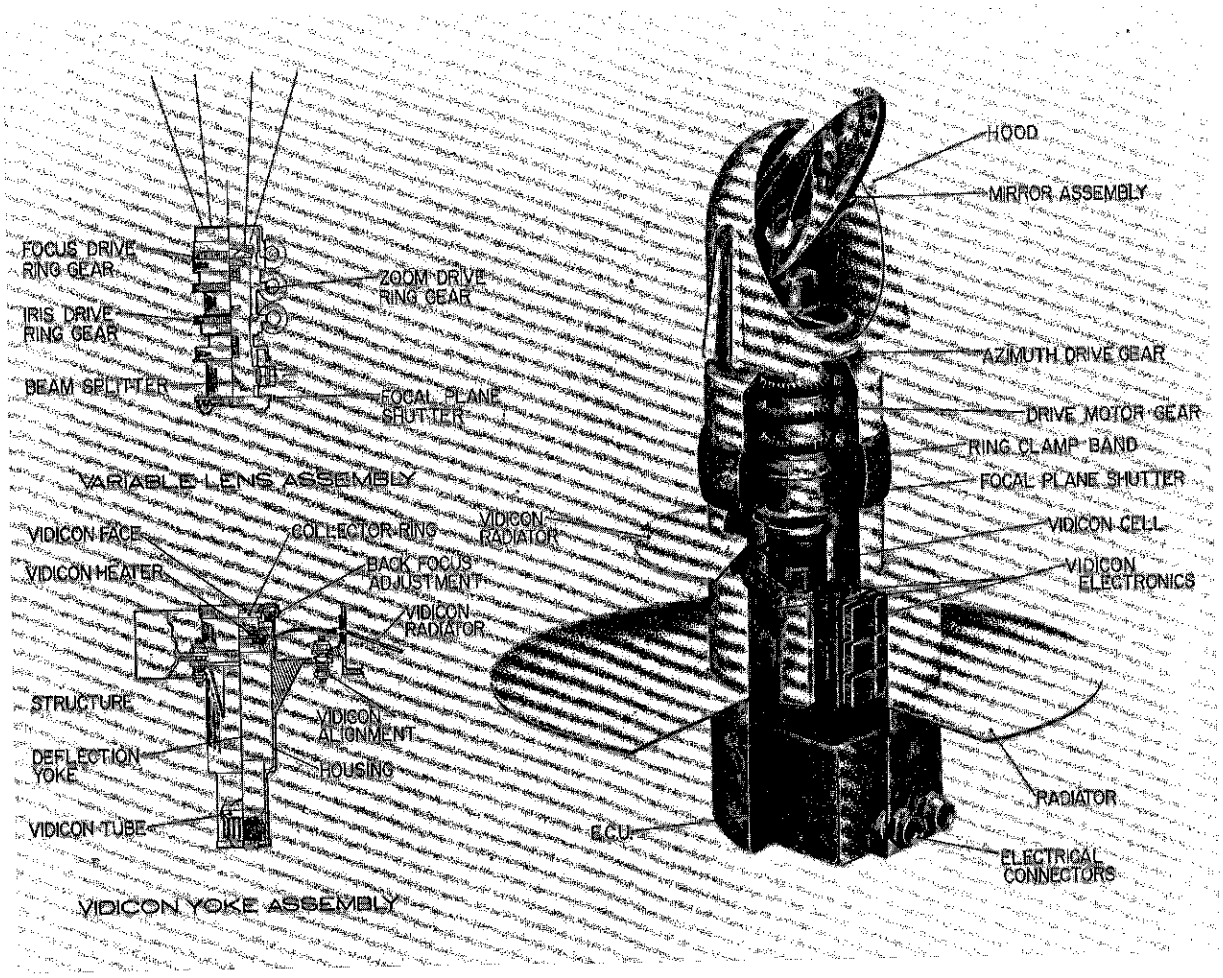

FIGURE 4. — Cutaway views of the survey television camera.

computer, autopilot, and vernier engines, provided automatic closed-loop guidance for final descent to touchdown.

Two propulsion systems were used by Surveyor I. The main retrorocket employed a solid propellant in a spherical steel case. Its thrust was of the order of 8000 to 10 000 pounds (35 500 to 44 500 newtons), depending upon temperature. The second, or vernier, propulsion system used hypergolic liquid propellants. The fuel was monomethyl hydrazine hydrate and the oxidizer was MON-10 (90 percent N_2O_4, 10 percent NO). Three throttleable thrust chambers were used, each capable of delivering from 30 to 104 pounds (133 to 462 newtons) of thrust as required by the flight-control subsystem. One chamber could be swivelled for roll control. The vernier engines were used for the midcourse maneuver and in the terminal lunar landing sequence.

For communications, Surveyor I carries two transmitters, two receivers, two omnidirectional antennas, and the planar-array high-gain antenna, used for transmission of the 600-line television pictures. Tracking and engineering data were transmitted continuously on a frequency of 2295 Mc at a power of 10 watts. The radio link also incorporates decoders that address commands received from Earth to the proper subsystems aboard the spacecraft, and signal processors that condition various data signals for transmission back to Earth.

The survey TV camera aboard the spacecraft

(fig. 4) transmits 200- and 600-line pictures of the lunar surface on command from Earth. The vidicon tube and its shutter, diaphragm, and optics are mounted nearly vertically, surmounted by a mirror that can be adjusted by stepping motors both in azimuth and elevation. Provision is also made for remotely inserting filters in the optical system, to permit colorimetric evaluation of individual pictures. The focal-plane shutter of the camera, normally providing an exposure time of 150 milliseconds, can also be held open for longer intervals on Earth command. A lens of variable focal length is used, covering a field of 6.4° by 6.4° at its maximum focal length of 3.9 inch (100 mm), and a field of 25.4° by 25.4° in its wide-angle focal length of 0.98 inch (25 mm). The focus distance of the lens can also be commanded to cover the range from 4 feet to infinity; and the diaphragm, though adjusted automatically, can also be set by command sent to the camera from Earth.

In addition, more than 100 items of engineering instrumentation were carried by Surveyor I and their readings telemetered to Earth. They include temperature sensors, strain gages, accelerometers, and position-indicating devices. The weight of this engineering payload, including an auxiliary battery, is 63.5 pounds (28.5 kg).

TRAJECTORY

SURVEYOR I WAS LAUNCHED ON MAY 30, 1966, from Complex 36-A of the Eastern Test Range. Its azimuth was 102.3°. The spacecraft was injected directly into its initial trajectory without the use of a parking orbit. A midcourse correction maneuver (fig. 5) was executed some 16 hours after launch (06 45 GMT, May 31) and the spacecraft was then returned to cruise mode. The autopilot and vernier propulsion system were used for this correction, which called for only a modest change in the predicted landing point.

As Surveyor I approached the Moon about 63 hours after its launching, a command from the Deep Space Network Station at Goldstone, California, modified the spacecraft's attitude to align the main retrorocket thrust axis along the path of flight (fig. 6). At an altitude of 59.35 miles above the Moon's surface, a signal from the altitude-marking radar mounted within the nozzle of the main retrorocket occurred, and 7 seconds later (at an altitude of 46.75 miles and a spacecraft velocity of 5839.87 mph) ignition took place, expelling this radar and initiating the 40-second main retrorocket burn. At the completion of this burn and jettisoning of the empty rocket case, Surveyor I was close enough to the Moon to receive an excellent return from its radar altimeter and Doppler velocity sensors. Operating in a closed-loop mode, these signals were processed by the on-board computer and autopilot to control the three vernier rocket engines, steering and decelerating the spacecraft in a predetermined optimum descent profile. Finally, at an altitude of about 14 feet, the vernier engines were cut off and Surveyor I dropped gently to the surface of the Moon at a speed of approximately 10 fps. It landed at a position (fig. 7) within about 9 miles (15 km) of the aiming point established at the time of the midcourse correction.

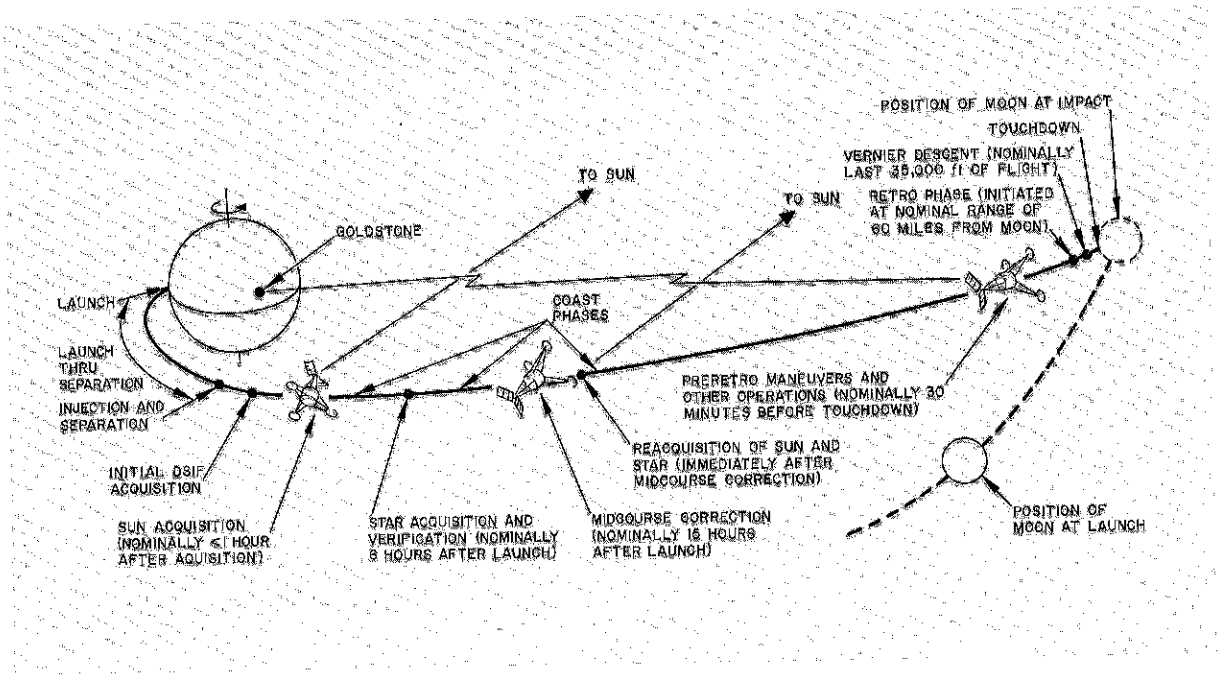

FIGURE 5. — Earth-Moon trajectory and nominal events.

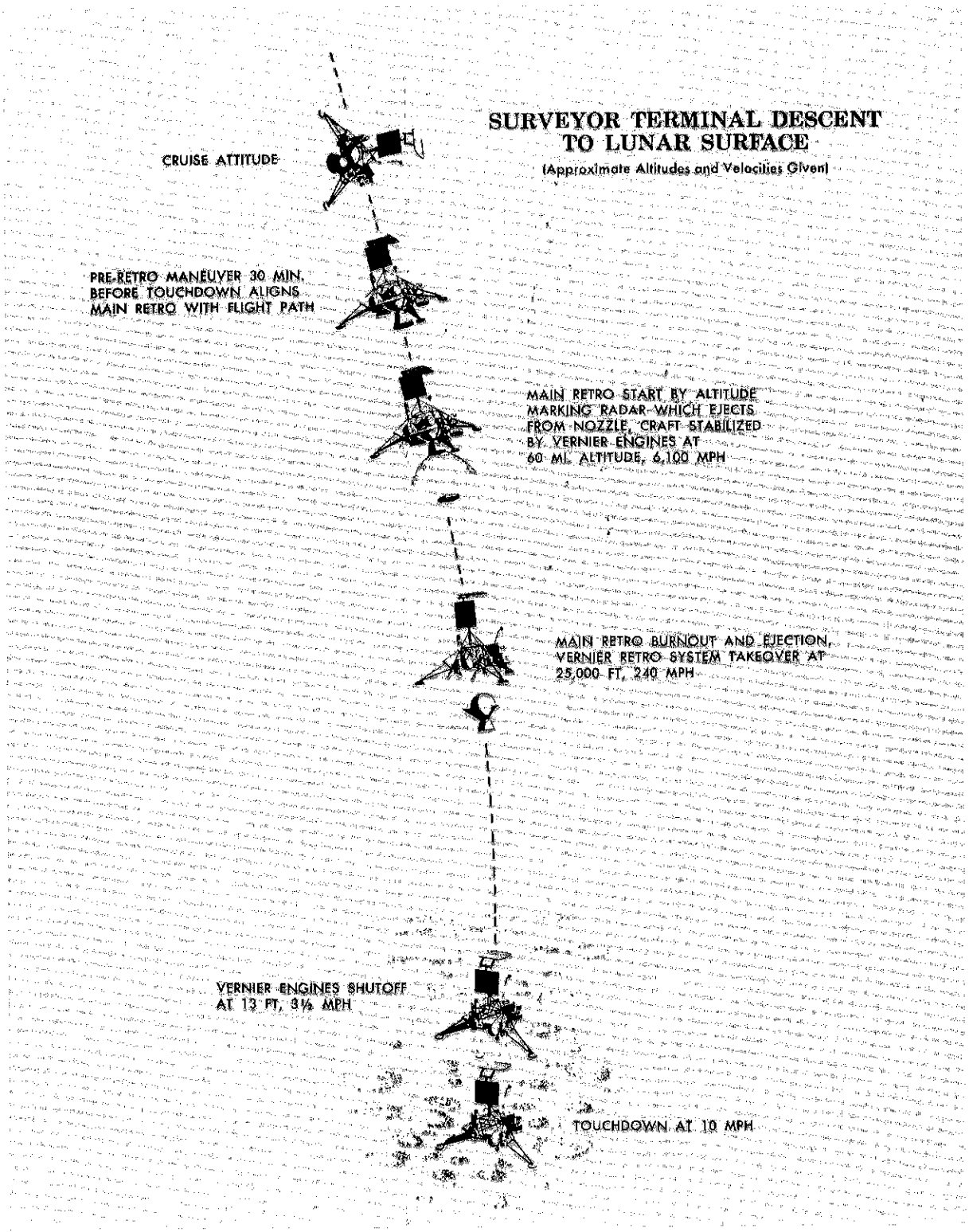

FIGURE 6. — Terminal descent and nominal events.

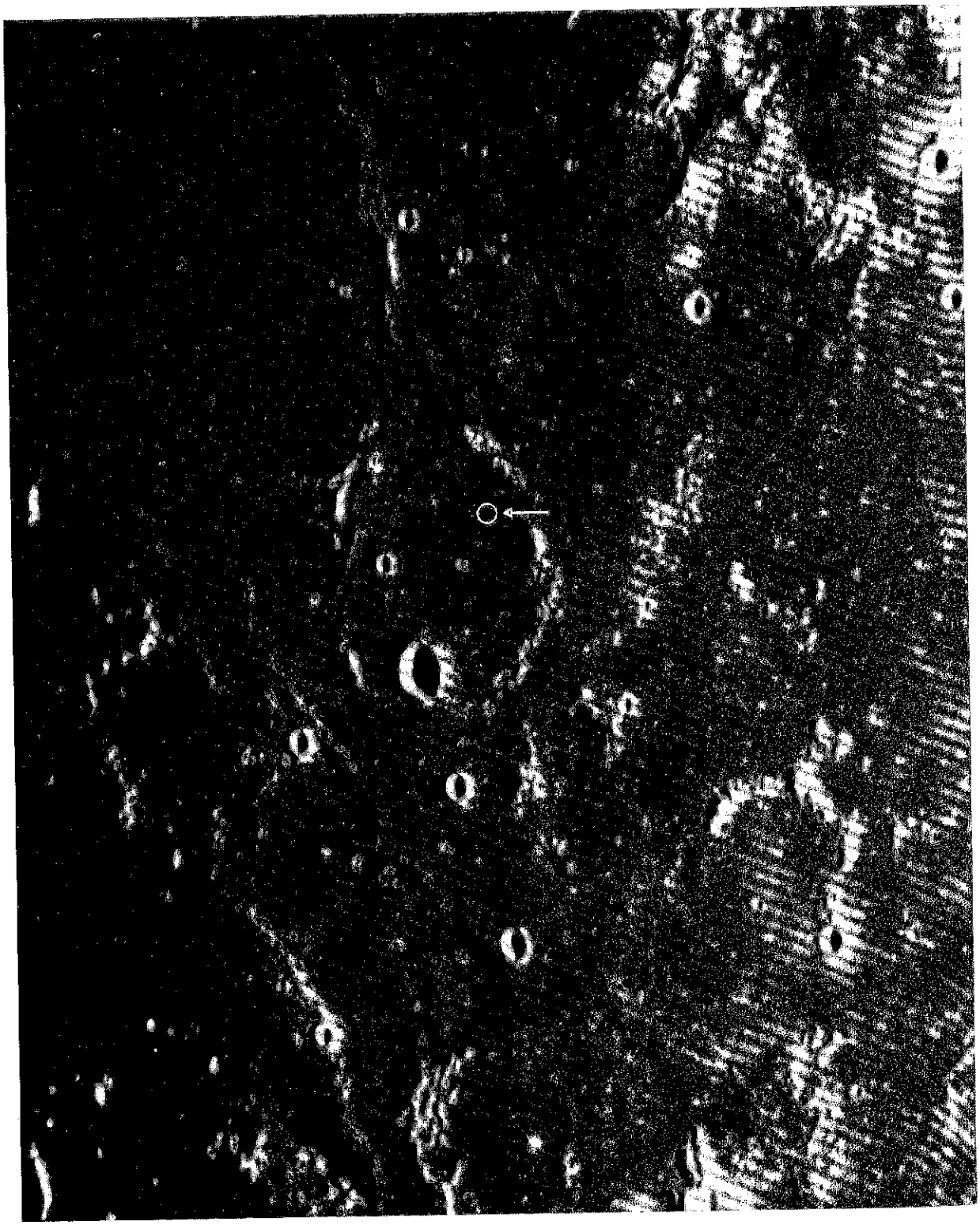

FIGURE 7. — Landing site of Surveyor I is some 35 miles north of the crater Flamsteed in Oceanus Procellarum. (Photo from McDonald Observatory, Fort Davis, Texas.)

TRACKING AND DATA ACQUISITION

DURING THE IMMEDIATE POSTLAUNCH PERIOD, tracking and telemetry were accomplished by Eastern Test Range stations at Cape Kennedy, Grand Bahama, Grand Turk, Antigua, Ascension, and Pretoria. The ships *Sword Knot, Coastal Crusader,* and *General Arnold* also acquired S-band telemetry data. The NASA Manned Spaceflight Network provided support from Grand Canary, Bermuda, Kano, Tananarive, and Carnarvon.

After the spacecraft separated from the launch vehicle, tracking and command functions for the rest of the translunar trajectory were the responsibility of the Deep Space Network (DSN) Stations at Goldstone, California; Johannesburg, South Africa; and Canberra, Australia. The midcourse and terminal maneuvers, and touchdown events, were tracked and commanded from Goldstone, which also served as the prime recovery station for television data. All three DSN stations recorded flight data during periods of spacecraft "visibility" from each station; and all tracking and telemetry data were sent to the Space Flight Operations Facility (SFOF) at the Jet Propulsion Laboratory in Pasadena, California, for reduction and analysis. The SFOF served as the focal point for the conduct of the Surveyor I mission and originated more than 100 000 commands to the landed spacecraft.

Lunar Surface Mechanical Properties

Observations and Explanations

THE INTERPRETATION of the lunar surface properties discussed here is based on the photographs showing the lunar surface area that was disturbed by the footpads and crushable blocks, and on the histories of the axial loads in the shock absorber on each of the three legs during the landing (see fig. 3). The important components of the landing-gear assembly are shown in figure 8, and their motions during landing are illustrated schematically in figure 9. The spacecraft landed at a vertical velocity of approximately 10 fps (3 mps), with a small component of velocity in the horizontal direction. At the present time, there is an uncertainty of several feet per second in all the velocity information.

Figure 10 shows the time records of the axial load as measured by a strain gage on each shock absorber. It can be seen that surface contact for all three footpads was almost simultaneous, indicating that the spacecraft mast (fig. 3) at touchdown was approximately normal to the surface. The footpads impacted at intervals of 0.01 sec. Footpad 2 touched first, followed by footpad 1 and then by footpad 3.

The record further shows that following the primary impact, the spacecraft rebounded clear of the surface, and a secondary impact occurred approximately 1.0 sec after the initial impact, indicating that the footpads rebounded about 2½ in. (6 cm) above the surface. The second impact developed maximum loads equal to approximately one quarter of the maximum loads developed during the initial impact. The maximum vertical load applied to the footpads by the lunar surface material during the initial impact was 400 to 500 lb, or 180×10^6 to 230×10^6

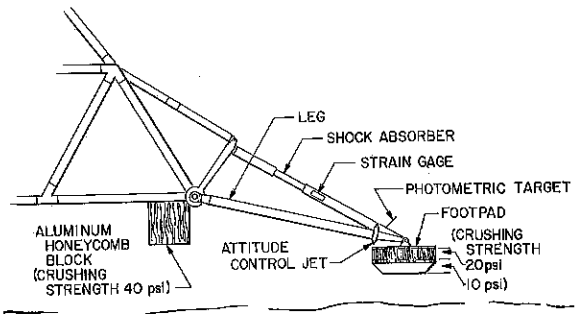

FIGURE 8. – Drawing of landing-leg assembly 2.

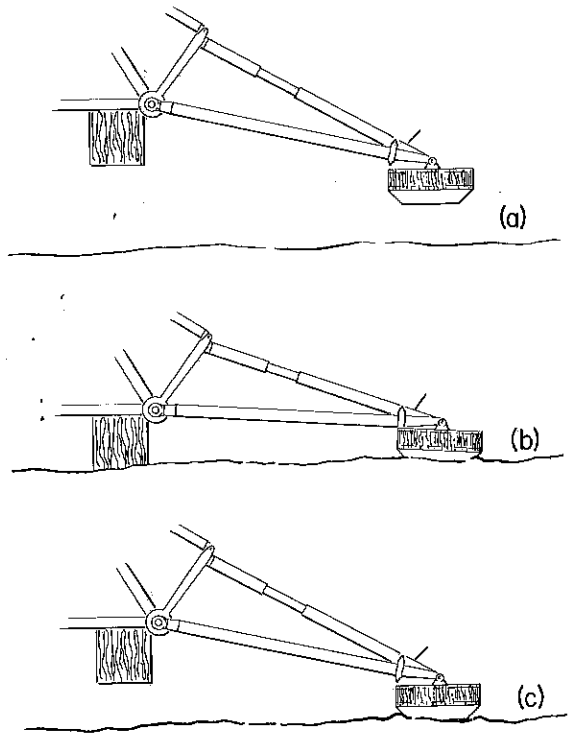

FIGURE 9. – Schematic of the Surveyor landing-leg assembly showing the articulation in a sequence of events during landing. In (a), the assembly is fully extended. During a landing, the shock absorber compresses and the footpad moves up and away from the spaceframe, as shown in (b). In (c), the assembly is shown reextended after landing.

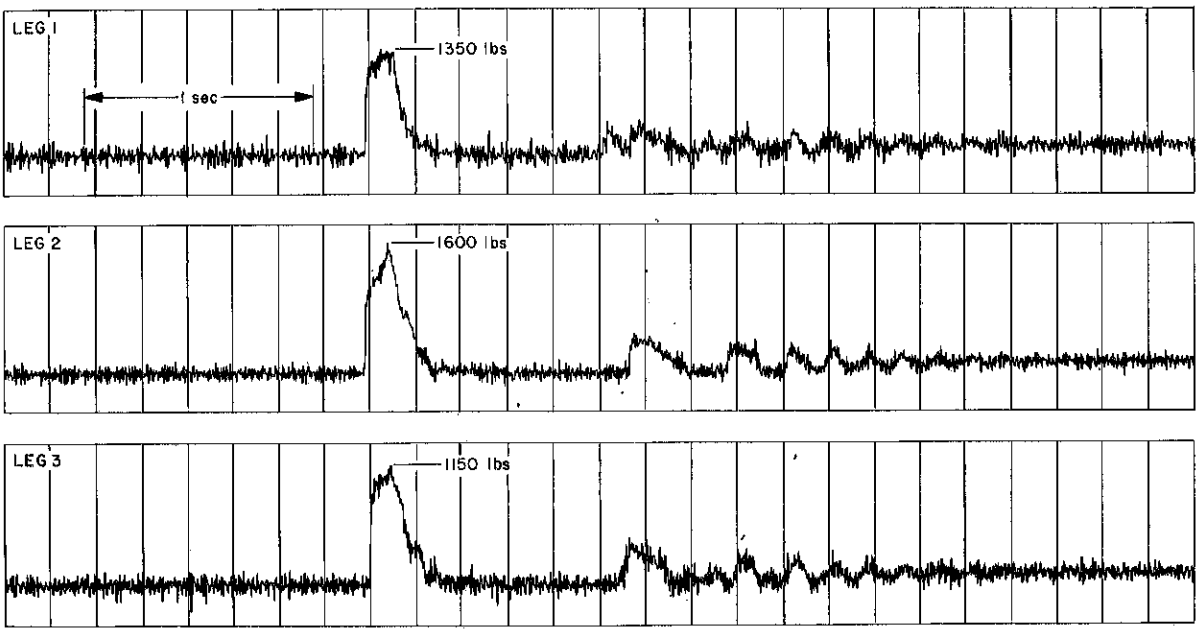

FIGURE 10. – Shock absorber strain-gage data as received at Goldstone, California. Note the oscillations following the primary impact.

dynes (1800 to 2200 newtons). Conversion of this load into a dynamic pressure applied to the surface depends on the footpad area in contact with the soil at the instant the load is measured. Since the lower portion of the footpad is a truncated cone (see fig. 8), this contact area depends primarily on the penetration depth. Based on the maximum vertical load and the footpad areas, a unit loading of between 4 and 10 psi (3×10^5 and 7×10^5 dynes/cm^2) was applied to the surface during the dynamic stages of the impact. The static load required to support the spacecraft on the three landing pads is about ½ psi (4×10^4 dynes/cm^2).

Based on preliminary velocity and spacecraft performance data, analytical simulations of the landing dynamics have been performed. To date, for simulated landings on a rigid surface, force levels have been duplicated within 10 percent. However, the timing of all events during the landing as indicated by the strain-gage data, i.e., rise time of force, rebound, reimpact, and durations of force during first and second impact, can be duplicated as precisely as the data allow it to be read out. The design of the spacecraft landing gear is such that the forces and motions of the spacecraft are largely independent of the mechanical properties of the surface for surface materials whose static bearing capacity is greater than approximately 5 psi (4×10^5 dynes/cm^2). Further discrimination of the material properties can be obtained from analyses of the footpad penetration.

A number of oscillations with a maximum peak-to-peak amplitude of several hundred pounds and a frequency near 7 cps are seen to follow the second impact (fig. 10). The oscillations of the forces in all the shock absorbers are in phase and of about equal amplitude, indicating a rectilinear vertical mode. The frequency of the oscillations is related to the elasticity of the spacecraft structure and the lunar surface material.

A picture of a depression in the lunar surface under cylindrical crushable block 3 (see fig. 11) indicates that it also made contact with the lunar surface. At the date of this writing, it has not been possible to identify positively any lunar surface depression under crushable block 1. The area beneath crushable block 2, and the crushable blocks themselves, cannot be seen with the Surveyor TV camera. However, the symmetry of the impact and the general local flatness of the

FIGURE 11. — Photograph of the surface depression made by crushable block 3. Note the depression made in the upper left-hand corner. Some parts of the spacecraft are shown.

lunar surface lead to the conclusion that all the crushable blocks made contact with the lunar surface. Measurements of shadows of the depression made by crushable block 3 indicate a depression depth of about ¾ in. (2 cm).

Pictures of each footpad confirm the nature of the landing expressed by the dynamics data. Pad 2 (fig. 12) and pad 3 (fig. 13) are both visible; pad 1 is not. The appearance of the lunar surface near pads 2 and 3 indicates similar behavior of the material displaced by the two pads. They appear to have landed in a granular material, to have extended laterally during impact (as shown in figure 9), forcing the surface material

FIGURE 12. — Wide-angle photograph of footpad 2. Note the displaced material that covers the lunar surface beyond the footpad, and the ray extending to the left from the footpad.

away, and then to have drawn back on the rebound to their final position, leaving a disturbed region of the surface.

There is no evidence to indicate crushing of the conical section of the footpad. At least the visible part of the lower layer, made up of aluminum honeycomb material having a crushing strength of 10 psi (7×10^5 dynes/cm^2), is undamaged (see fig. 14). No crushing of the upper layer of crushable structure (crushing strength of 20 psi, or 1×10^6 dynes/cm^2) took place. It should be noted that, at the landing velocity of approximately 10 fps (3 mps), preflight analyses have shown that no crushing of the footpads would occur even on a rigid surface. This would indicate that dynamic pressures of 10 psi (7×10^5 dynes/cm^2) on the footpads during landing were not exceeded and that the footpad did not crush, but displacement of the granular surface material occurred. The shock-absorber data, as discussed above, are in agreement with this evaluation.

At both pads 2 and 3 there is a throwout pat-

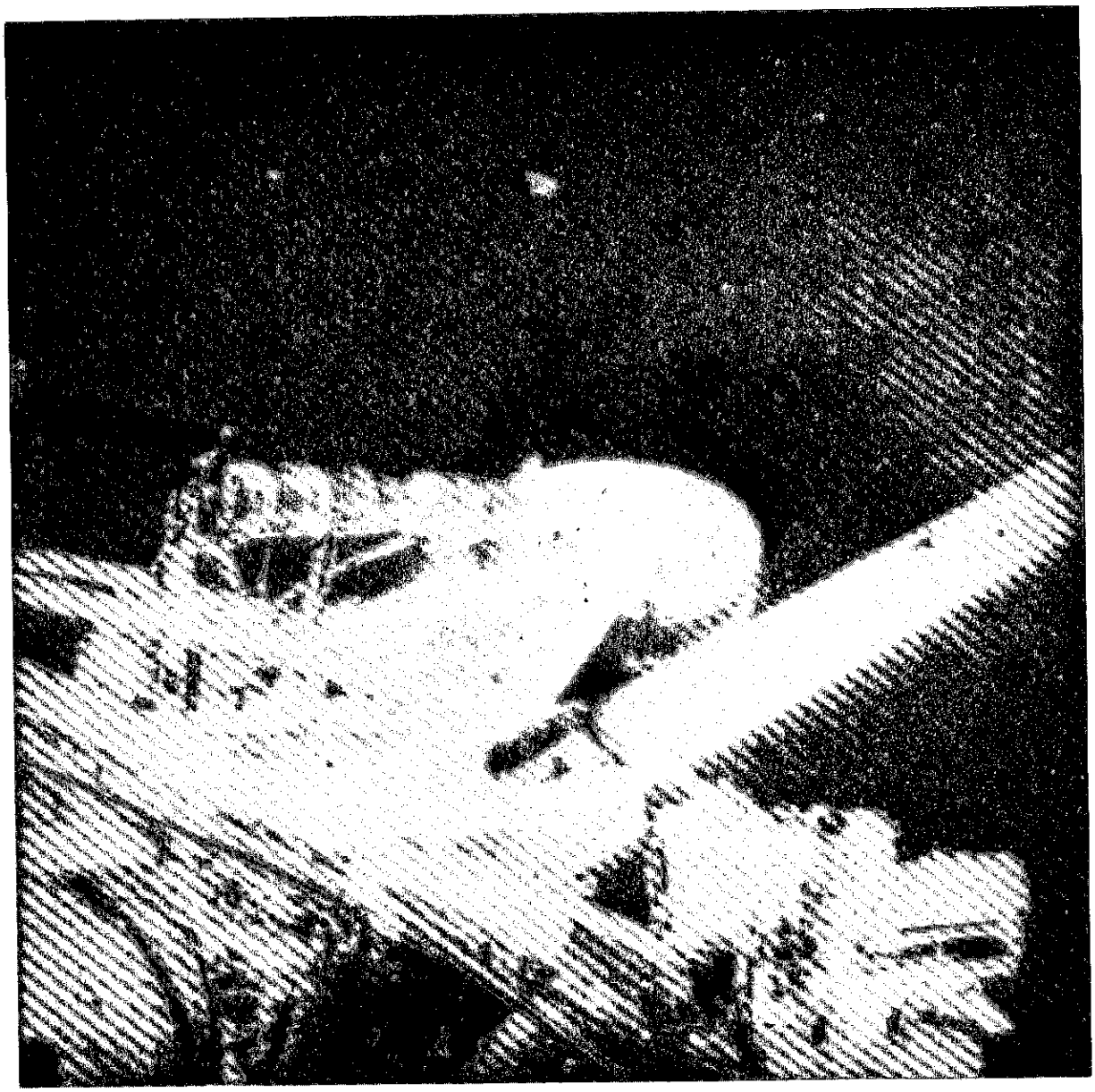

FIGURE 13. – Wide-angle photograph of footpad 3. Note the similarity of the throwout material to that shown in figure 12.

tern over the surface (see figs. 12 and 13), including rays of apparently fine-grained material, to a distance of a foot or two from the edge of the pad. Nearer the pad, the surface material is pushed up by the impact to form a raised rim. The side of the depression and the rim have a chunky or blocky appearance (fig. 15); the blocks or clumps of material are irregular, have a range of sizes, and appear to consist of aggregates of fine-grained material rather than of individual stones or pebbles. The basic grain size is quite small and below the limit of resolution of the narrow-angle pictures in the 600-line mode. The limit is about 0.02 in. (0.5 mm) at the distance of pad 2.

Pad 2 movements during landing caused some

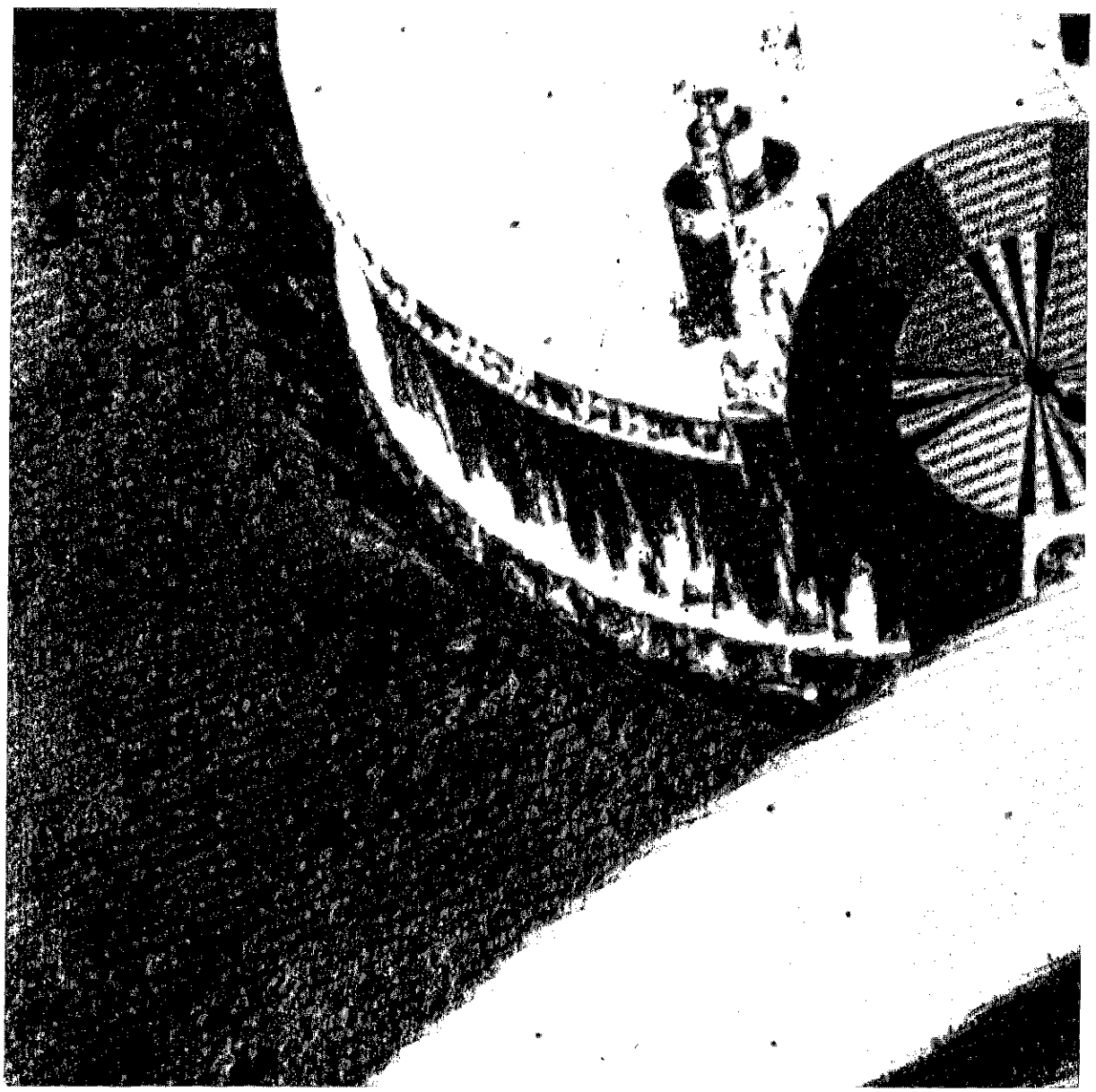

FIGURE 14. – Narrow-angle photograph of footpad 2. The upper part of the pad is made of honeycomb structure having a crushing strength of 20 psi (1×10^6 dynes/cm^2). The lower part has a crushing strength of 10 psi (7×10^5 dynes/cm^2). The photo was digitized and corrected for system frequency response by G. Smith, R. Selzer, and F. Billingsley, Jet Propulsion Laboratory. Grains of 0.5 mm can be resolved in the disturbed surface next to the footpad.

small deformations of the surface adjacent to the pad on the side nearest the camera (fig. 16). The deformations resulted in an irregular pattern of cracks or fissures at the surface of the material. The pictures of pad 2 (e.g., fig. 12) clearly show that its cylindrical part lies above the level of the undisturbed surface. The penetration of pad 2, in the final location, was calculated from shadow measurements on two photographs taken 69 hr apart. The measurements indicate that the base

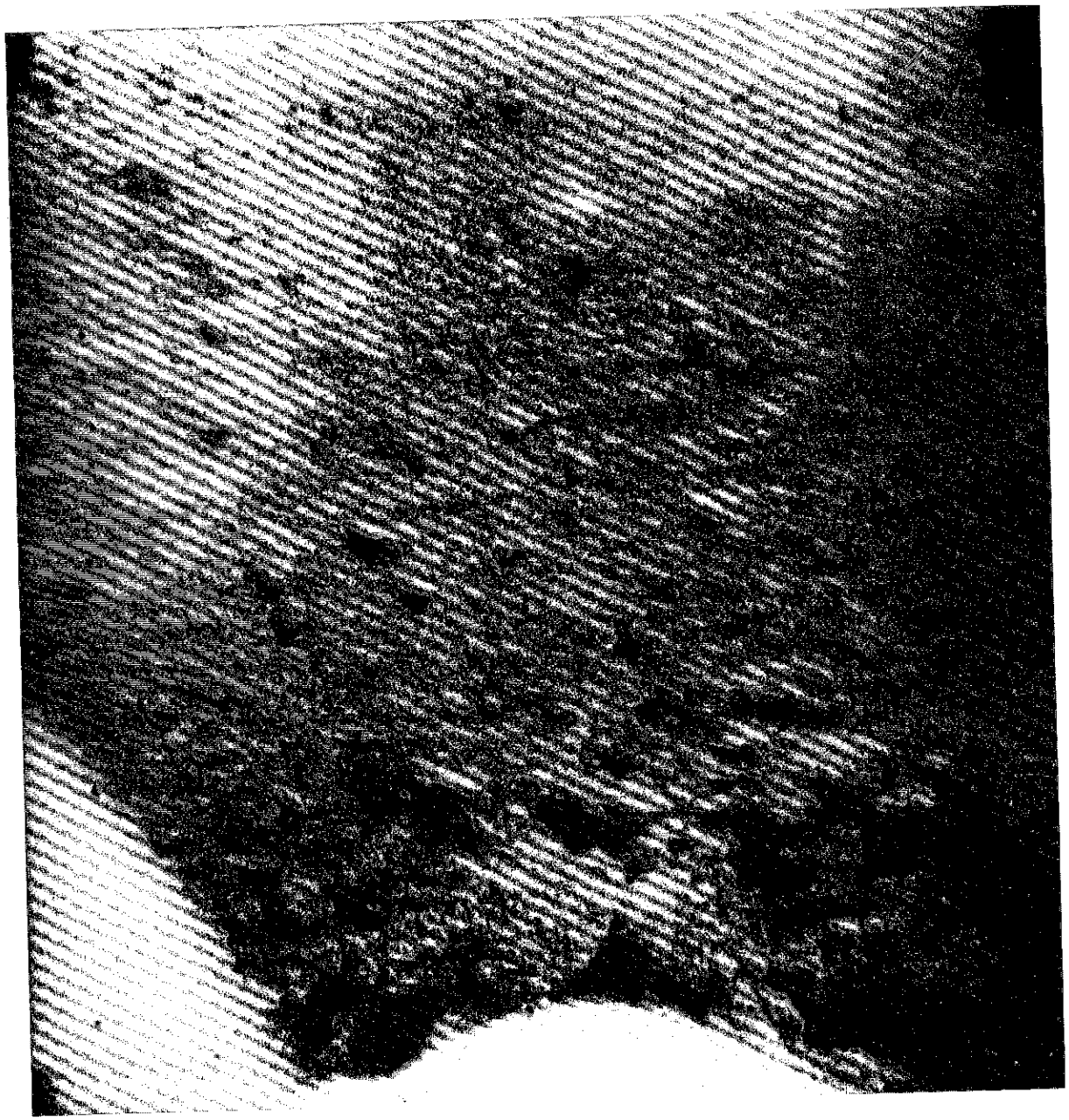

FIGURE 15. – Narrow-angle photograph of the disturbed lunar material beyond footpad 2, which is the circular object at the bottom of the picture.

of the footpad, if it is uncrushed, lies about 1 in. (25 mm) below the adjacent undisturbed surface.

Until a detailed study of the depression caused by the pad is completed, it is not possible to say to what extent the lunar surface material was actually compressed in volume by the impact. It is certain that the craters caused by the pad impacts did not result entirely from volumetric compression and that some displacements of the material did occur.

To determine whether any surface erosion could be caused, the attitude-control jet on leg 2

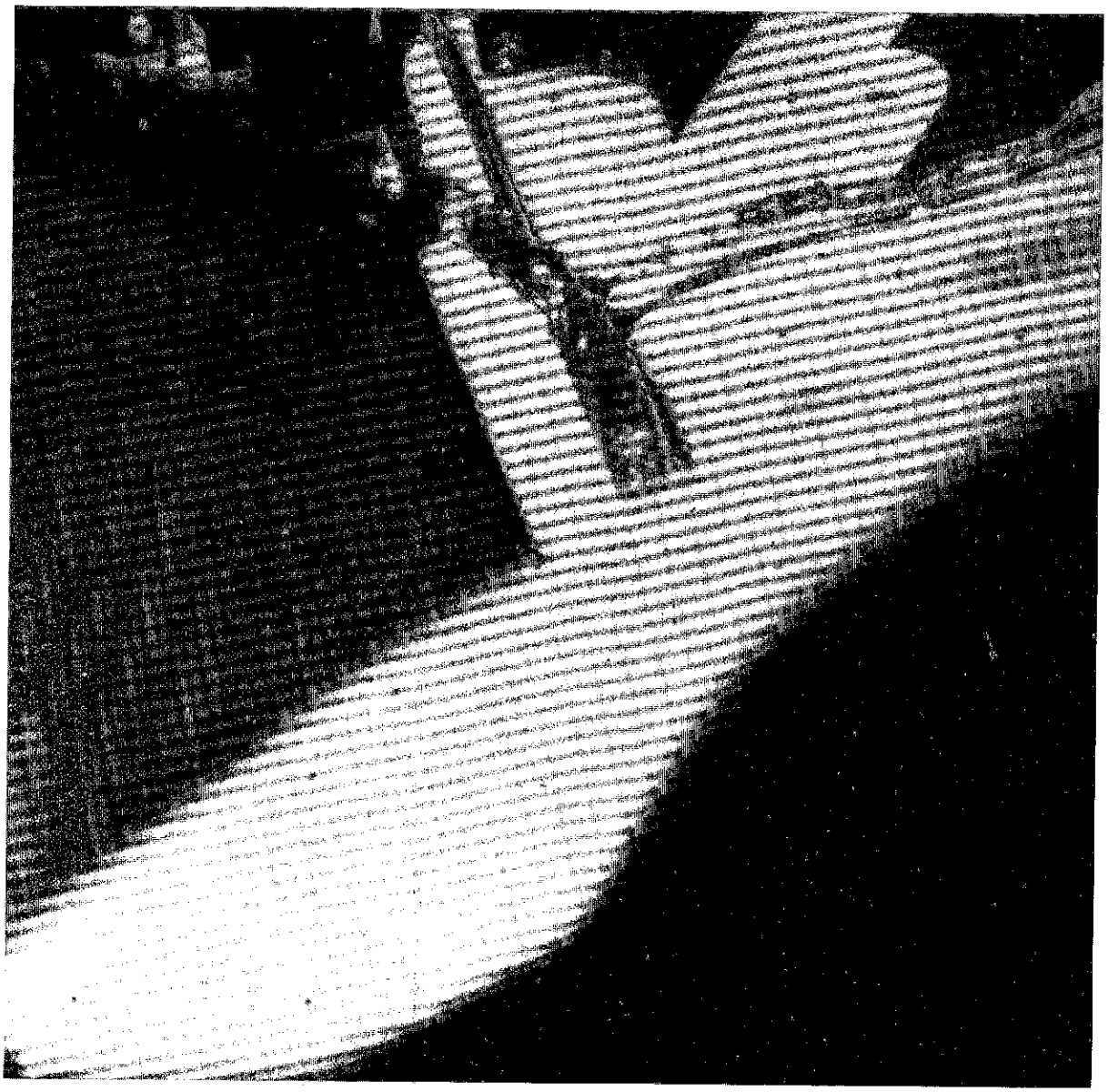

FIGURE 16. – Narrow-angle photograph of the disturbed lunar surface material near footpad 2. The pad is in the upper portion of the photograph; the surface shown lies between the footpad and the spaceframe.

(fig. 8) was operated after landing. This jet uses cold nitrogen gas to produce a thrust of 0.06 lb. It was located approximately 6 in. (15 cm) from, and at an angle of 72 deg to, the surface. Pictures were taken before, during, and after the firings, which consisted of short pulses repeated for periods up to 4.5 sec. The duration of the pulses was 20 msec with a 30-msec pause between pulses. At the present time, results of this experiment are inconclusive, since the initial study of the pictures taken before and after the firings did not indicate any obvious soil disturbance. A more detailed study of these pictures remains to be made.

Interpretations

The appearance of the disturbed surface material and the rim of the impact depression suggest that the surface is a granular soil-like medium of unknown but fine grain size and size range. On disruption by the impact, some fine-grained material was thrown out in a spray, possibly from an original surface layer, and the underlying material was broken up to some extent.

The behavior of the material is consistent with its possession of a distinct but small amount of cohesion, and its manner of deformation appears to be qualitatively similar to that which might be exhibited by a terrestrial, damp, fine-grained soil.

The appearance of the lunar surface and the nature and depths of the depressions formed during landing are very similar at pads 2 and 3, so that, at least to the scale of Surveyor, the material properties appear to be horizontally homogeneous.

If, to a depth of the order of the footpad diameter (1 ft, or 30 cm), the material is homogeneous and similar to that observed at the surface, a simplified landing dynamics analysis indicates that the soil has a static bearing capacity, at the scale of the Surveyor footpad, of about 5 psi (3×10^5 dynes/cm^2).

Although this bearing capacity can be developed by materials having a wide range of properties, a reasonable choice, considering all the available data, is a soil with a cohesion in the range of 0.02 to 0.05 psi (1×10^3 to 4×10^3 dynes/cm^2) and a friction angle between 30 and 40 deg, at a density typical of terrestrial soil (3 slugs/ft^3 or 1.5 g/cm^3).

However, the landing dynamics data, penetration observations, and landing simulations performed to date are also compatible with a lunar surface consisting of a hard material (static bearing capacity greater than 10 psi, or 7×10^5 dynes/cm^2), overlain by a weaker material, to a depth of about 1 in. (25 mm).

Lunar Surface Thermal Properties

Earth-Based Observations

THE LANDING SITE OF SURVEYOR I, 2.4° S latitude and 43.3° W longitude, is contained in the Lunar Isothermal Chart (ref. 1). The site is in a "bland" area, in that local surface temperature gradients across the surface during lunar eclipse are small; this is typical of the major portion of the visible lunar surface. A further characteristic of these typical areas is that the surface exhibits a high value, of the order of 800 cgs units, of the thermal parameter $(k\rho c)^{-1/2}$, where k is thermal conductivity, ρ is density, and c is specific heat. For comparison purposes, an evacuated powder consisting of 1- to 25-μ-sized particles of olivine, tektite, or granodiorite has a thermal parameter in this range (ref. 2). It is interesting to note that the measured bearing strength of such powders is sufficient to be consistent with that of Surveyor I resting on the lunar surface (ref. 3). Further, the site is in a relatively dark area, where the albedo or solar reflectance is lower than the average. (J. M. Saari estimates the local albedo to be 0.052.)

Observations Based on Spacecraft Data

A rather firm conclusion can be drawn from temperatures at many locations throughout the spacecraft during its operation on the lunar surface. The spacecraft temperatures are at levels to be expected with clean external thermal-radiating surfaces. This strongly indicates that the surfaces have essentially no dust on them. It should be noted that thermal conditions of the lunar surface have little effect on temperatures at most spacecraft locations because the underside of the spacecraft has a highly reflecting metallic surface.

The temperatures of a few of the external surfaces on Surveyor I are determined primarily by heat exchange with the lunar surface and with deep space. These spacecraft surfaces are rather well insulated, in terms of both conduction and radiation, from the remainder of the spacecraft. The portion of the lunar surface which determines the spacecraft temperatures is very localized: 80 percent of the radiation view factor from the selected spacecraft surface to the Moon is made up of approximately 1000 ft^2 (100 m^2) adjacent to the spacecraft.

A very preliminary estimate of the lunar surface brightness temperature at 1200 GMT, June 2, 1966, is 180° F. (ref. 4). This estimate, based

on measured spacecraft temperatures, is for the appropriate Sun elevation angle of 31 deg and an assumed lunar surface thermal emittance of 1.0. The value of 180° F. may be compared with a preliminary prediction of a local lunar surface brightness temperature of 130° F. derived from Earth-based measurements. Simplified thermal models of both the spacecraft and the lunar surface were used in making these estimates. A much more detailed analysis is necessary before it can be confirmed that the local surface temperature of the Moon, at the Surveyor 1 landing site but without effects introduced by the spacecraft, is warmer than the average for that portion of the Moon.

Lunar Surface Topography and Geology

Introduction

FOUR THOUSAND PICTURES were taken with the television camera on the Surveyor I spacecraft during the first five days after landing. During this period, the lunar surface was observed through Sun elevation angles ranging from 28 to about 88 deg. An immense quantity of detailed information about the local lunar surface is contained in the pictures; we report here the first scientific results obtained from the forenoon and lunar noon photographs.

The Surveyor television camera was operated in two modes: one in which the picture is composed of 200 television scan lines, and a second higher-resolution mode in which the picture is composed of 600 scan lines. A total of 14 pictures in the 200-line mode and 3986 in the 600-line mode were obtained. The 600-line Surveyor television pictures are of superior quality and may be compared favorably with the lunar television pictures acquired by the Ranger spacecraft. The Surveyor pictures are exceptionally free of coherent noise and show very little shading of the field, owing to the relatively uniform response of the vidicon target.

The calibrated angular resolution of the Surveyor camera (½ mr at 15 percent relative response) is about half the angular resolution of the average human eye. The ground resolution near one of the spacecraft footpads, about 1.6 m from the camera, as measured from pictures for which the modulation transfer function has been compensated (fig. 14), is about 0.5 mm. Higher ground resolution can be achieved directly beneath the camera. It is of interest to note that the highest resolution obtained in the Ranger pictures represents an improvement over the best resolution of the lunar surface achieved at the telescope by three orders of magnitude, and that the Surveyor pictures represent a gain in resolution over the highest-resolution Ranger pictures by an additional three orders of magnitude. The Surveyor I television pictures exhibit a significant gain in resolution over the pictures acquired earlier this year by the Soviet spacecraft Luna IX.

The total range of response of the Surveyor I camera is about 1 000 000 to 1, enabling its use for recording stars as faint as sixth magnitude, on the one hand, and for photographing the brightest parts of the lunar surface on the other. Thus, the dynamic range of the Surveyor camera is within a factor of ten of the dynamic range of the human eye.

The photometric response of the Surveyor I camera on the Moon, observed by means of repeated pictures of a photometric calibration target mounted on a leg of the spacecraft, has proved to be fairly stable and close to the response observed in preflight calibration. In its normal mode of shutter operation, which provides a 150-msec exposure, the total dynamic range of the vidicon tube is approximately 25 to 1; the logarithm of the video voltage is nearly a linear function of the log lunar scene luminance over a range of about 5 to 1 (fig. 17).

The great dynamic range of the camera system is achieved by means of an iris, by filters in the optical train, and by alternate modes of shutter operation and electron-beam scanning cycle. By use of the variable iris aperture, which provides nominal focal ratios ranging from f/4 to f/22, the dynamic range of the camera is increased from 25 to 1 to somewhat more than 800 to 1. Rotation into the optical train of color filters on a camera filter wheel can be used to increase further the dynamic range to about 3000 to 1. By use of a 1.2-sec. exposure (open shutter mode), the dynamic range of the camera

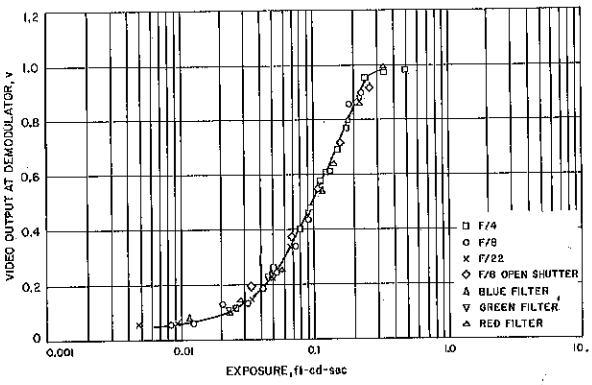

FIGURE 17. — Calibration data for the Surveyor I television camera illustrating dynamic range.

can be extended to about 25 000 to 1. Finally, the sensitivity of the camera to very faint objects can be increased still further, by a factor of about 40 over the open shutter mode, by means of several minutes' exposure (integration mode).

The color filters in the camera filter wheel were selected so that the overall camera-filter spectral response (fig. 18) would match the standard color matching functions of colorimetry

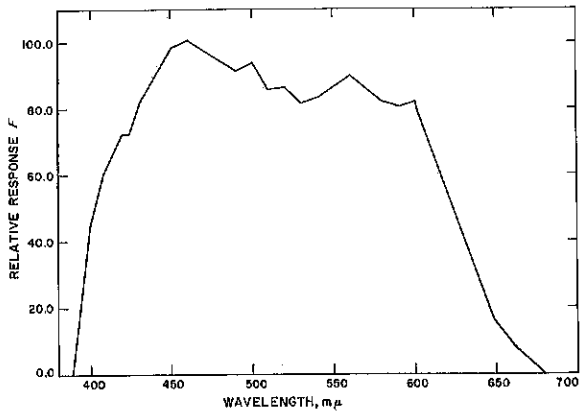

FIGURE 18. — Spectral response curve of the Surveyor I television camera, at the clear position of the filter wheel.

as well as is possible with single filters (fig. 19). In order to maintain colorimetric calibration and enhance the detection of color differences, the photometric target is equipped with three colors of purity and dominant wavelength that bound the gamut of normal rock colors. Figure 20 shows the appearance of the target as seen on the lunar surface through the three color filters.

The lens assembly of the Surveyor television camera is constructed to provide a variable focal length, ranging from 25 to 100 mm. The camera is normally operated at either the long or short focal-length extremum, the 25-mm focal length resulting in a 25.4-deg optical field of view, and the 100-mm focal length resulting in a 6.4-deg field of view. For convenience, we refer to the former as a wide-angle frame and to the latter as a narrow-angle frame.

The camera has been operated to provide a wide variety of information (table 1). Several wide-angle frame panoramas have been taken of the lunar scene on different days and with different color filters. (A complete wide-angle frame panorama requires about 120 frames.) Several sectors of the complete panorama have also been taken in narrow-angle frames on different days and with color filters. (A complete narrow-angle frame panorama requires nearly 1000 frames.) Surveys of two of the spacecraft footpads and of imprints on the lunar surface left by the crushable blocks beneath the frame of the spacecraft have been conducted on each

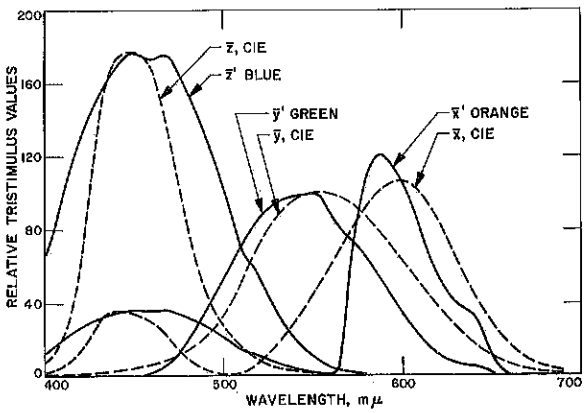

FIGURE 19. — Graph of the overall camera-filter spectral response illustrating the fit to the standard CIE (Commission Internationale l'Eclarage, 1931) color-matching functions. The second maximum in the $\bar{x}'$ curve is obtained from a reduced value of the $\bar{z}'$ function added to the original $\bar{x}'$ camera-filter response. Solid lines are camera-filter response curves; dashed lines are CIE color-matching function.

TABLE 1.— *Categories of television pictures taken during lunar forenoon and noon*

	Approximate number of frames
200-line pictures	14
600-line pictures	
Wide-angle frame panoramas	390
Narrow-angle frame panoramas	1160
Wide-angle frame panoramas with color filters	870
Narrow-angle frame panoramas with color filters	1160
Footpad survey	100
Crushable block imprint survey	30
Gas jet experiment	30
Star survey	20
Photometric and color calibration target	100
Study of objects of special interest and verification frames for aperture, focus and position	126
TOTAL	4000

successive day. On two days, the attitude-control jets mounted on the legs of the spacecraft were fired, in an experiment to determine whether the gas emitted would disturb the surface; the effects were searched for by comparison of television pictures taken during and after the firing of the jets with pictures taken before. Repeated photographs were taken of the photometric and color calibration target each day to provide control for the photometric reduction of the pictures. Finally, several objects of special interest, such as large rocks close to the spacecraft, were examined with additional photographic coverage, in order to provide maximum information on the shape, texture, and color of these objects.

In order to measure the photometric function of the local lunar surface and various objects on the surface, and to map the surface topographically by use of shadows and by photometric techniques, it is necessary to survey the surface repeatedly at different positions of the Sun. Different kinds of information are provided about the surface, furthermore, at different angles of solar illumination. The fine texture and very shallow relief features are best shown at glancing solar illumination, whereas differences in albedo and color are best determined when the Sun is high, or when the phase angle of a given image element is very

FIGURE 20.— Photometric target on footpad 2 of the Surveyor spacecraft. The target is used for photometric calibration of the television camera during lunar operation. Frame (a) is observed through $\bar{x}'$ filter, (b) is observed through $\bar{y}'$ filter, and (c) is observed through $\bar{z}'$ filter.

small. Although 4000 pictures have been acquired at the time of writing, the photographic data are far from complete, and many thousand additional pictures will be needed to investigate thoroughly the features of interest in the field of view.

Location of the Spacecraft from Landscape Features on the Horizon

At least six features on the Surveyor panorama pictures can be identified as elevated terrain lying at a greater distance than the ordinary near horizon of about 2 km. A low mountain ridge to the northeast is the outstanding example. The ordinary near horizon in front of the distant features can generally be identified as a relatively sharp demarcation between the foreground and the distant elevated terrain, which is brighter and smoother in silhouette. All of the distant features recognized are concentrated in the northern part of the horizon. Figure 21 shows a mosaic of the horizon between northwest and northeast, with the features identified. Their characteristics are summarized in table 2.

TABLE 2.—*Characteristics of horizon features*

Feature	*Location, deg*		*Width visible*		*Maximum height visible*	
	Camera coordinate	*Approximate selenographic coordinate*	*deg*	*km**	*deg*	*m**
A	65	N 27° E	11.2	2.54	0.44	100
B	98.2	N 6° W	2.5	0.79	0.24	75
C	102.0	N 10° W	0.3		0.08	
D	105.8	N 13° W	1.5	0.52	0.15	52
E	124.0	N 32° W	0.5		0.12	
F	88.0	N 3° E	0.5	0.15	0.04	10

* The figures for the width and height of the features are for the parts visible over the horizon. They are calculated on the basis of the Site I location (see text).

The occurrence of the distant horizon features is consistent with the general location of the Surveyor landing site in the northeast portion of a plain north of Flamsteed encircled by hills and low mountains. In this area, there are several specific sites in a circular region of approximately 7-km radius from which most of the observed features can be explained by telescopically observed local lunar topography. Table 3 gives the location of two of the sites.

TABLE 3.—*Location of two possible solutions for the landing site of Surveyor I on the basis of horizon features in the landscape*

Site	*South latitude, deg*	*West longitude, deg*
I	2.15	43.35
II	2.49	43.32

Figure 22 shows the location of these sites on a Lunar Chart and illustrates, for the case of Site I, the degree to which the horizon features observed by Surveyor can be explained by known mountains. Site II coincides with the site deduced from trajectory tracking data. It is presented in figure 22 with an ellipse showing the 2-σ uncertainty in its location based on a preliminary reduction of the tracking data. Among the sites studied, Site I appears somewhat preferable from known features of the lunar landscape. It best explains the most prominent feature, A, even though the two minor features, C and E, are not explained in detail.

At present, it is not clear whether the disagreement (about 5 km outside the 2-σ error ellipse of the solution obtained from tracking) between the site deduced from trajectory tracking and the preferred site determined from topography is to be taken as a cause for concern. It is to be expected that later pictures of the horizon features and comparison with telescopic or Lunar Orbiter photographs of this region will provide sufficient data for a much more precise location of the landing site of Surveyor with respect to known selenographic features.

Slope of the Surveyor I Landing Site on the Kilometer Scale

The position of the horizon on the Surveyor panoramic pictures (particularly in the narrow-angle frames), together with the calibrated camera pointing angles, can be used to establish the local average inclination of the landing site

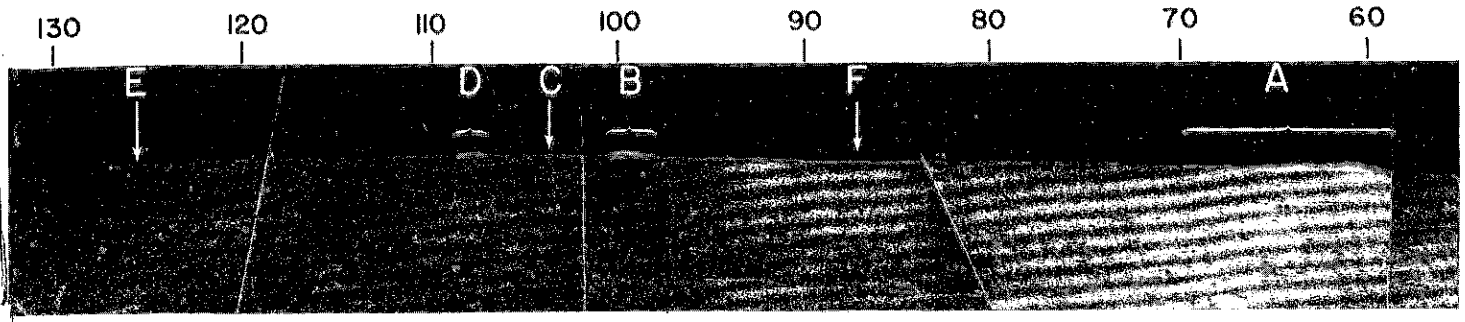

FIGURE 21. — Wide-angle panorama of the lunar horizon in the northern quadrant as observed by Surveyor I. The region covered is from 55 to 130° azimuth (camera coordinates); Sun elevation is approximately 50°. Most of the curvature of the horizon arises from the nonvertical mounting of the camera.

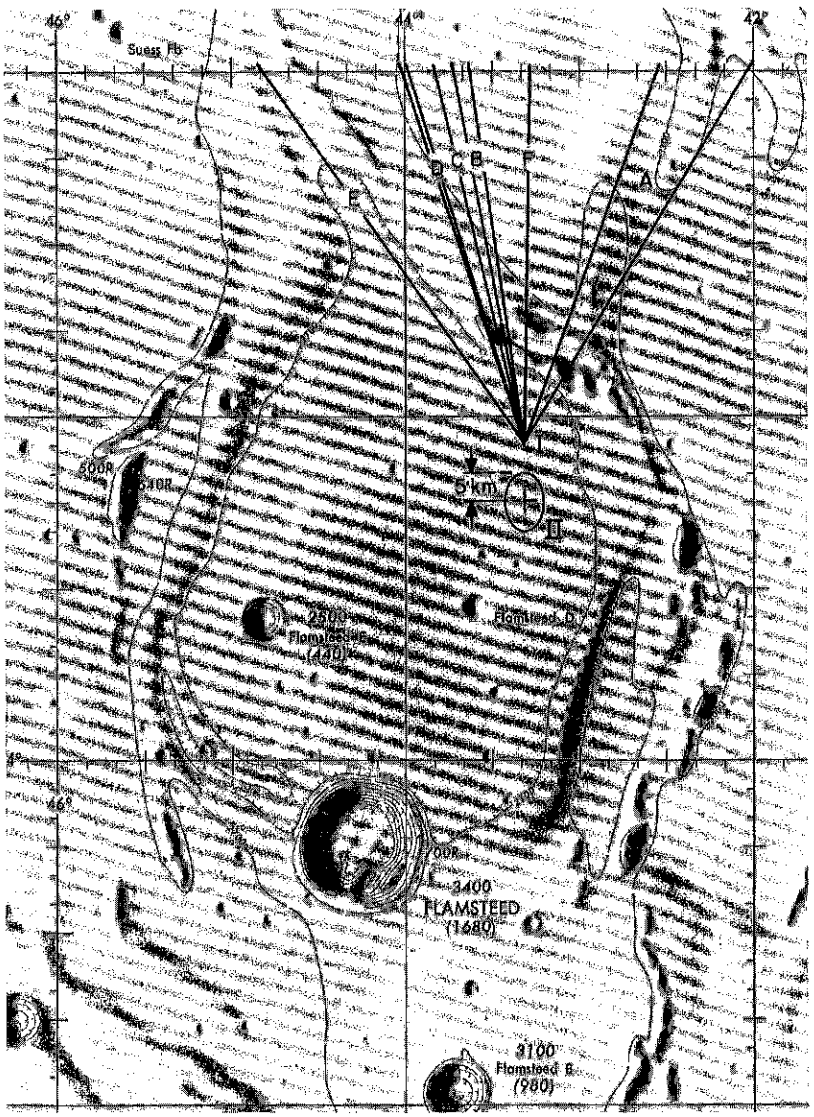

FIGURE 22. — Surveyor I landing sites as deduced from horizon features. Two sites that seem compatible with these features are shown. Site II coincides with the site deduced from trajectory tracking data. The ellipse around Site II is the 2-σ error. Base map—ACIC Lunar Chart LAC 75.

terrain relative to the spacecraft axis. This inclination can be determined to a fraction of a degree, and, if the horizon is relatively distant, applies on a kilometer scale.

Observations of the horizon positions can be converted to true slopes of the terrain once the attitude of the spacecraft relative to the local astronomical vertical is known. This is determined, in turn, by using the television camera to take star pictures. For this purpose, the camera was used in an open shutter mode. The relatively high luminance of the lunar terrain, however, resulted in a high background in daytime measurements. So far, the images of two stars, Sirius and Canopus, have been obtained. Rough analog reduction of the stellar position data shows that the spacecraft axis is tilted from the astronomical vertical by 1.7 ±0.5 deg in a direction a little south of east. Repeated observations of points on the horizon show that the spacecraft cannot have shifted attitude more than a few tenths of a degree since the first day after landing. Observation of the landing pads suggests that they penetrated the surface nearly equally. This implies that the spacecraft tilt is close to the slope of the lunar surface immediately beneath the spacecraft.

A detailed examination of the horizon positions, corrected for this spacecraft tilt, has been made for 65 directions over a range of azimuth of 250 deg extending from the north to the southwest. The results show that the Moon, at the Surveyor I landing site, is both relatively smooth and nearly level on a kilometer scale. The standard deviation of the angle to the horizon is only 0.7 deg. The average horizon position in the three quadrants examined is the same within 0.5 deg. More refined treatment of the observations can be expected to reduce the standard deviation.

General Morphology and Structure of Terrain Around the Spacecraft

Surveyor I is resting on a part of Oceanus Procellarum partially enclosed within a circle of hills and small mountains on the rim crest of an ancient crater that is almost completely buried beneath the mare material of the Oceanus. This ancient crater is about 100 km in diameter. The landing site is along the east border of a dark patch on the mare surface, which is the smoothest part of the mare within the mountain circle. The nearest small crater that can be easily resolved at the telescope is about 1 km in diameter and lies about 10 km to the east of our best estimate of the landing site.

The terrain within 1 to 2 km surrounding the landing site, as observed from the Surveyor pictures, is a gently rolling surface studded with craters ranging in diameter from a few centimeters to several hundred meters. Several craters that probably range in size from a little less than 100 m to perhaps as much as ½ km have been recognized along the horizon. Their true diameters cannot be accurately estimated. They range in angular width from about 15 to 36 deg. One of these craters, which lies slightly south of east of the spacecraft, has a prominent raised rim about 5 to 10 m high (fig. 23). The exterior slopes of this crater rim exhibit a maximum inclination to the horizon of about 11.5 deg. The visible rim crest and exterior slopes of the rim are strewn with coarse blocky debris. Two larger but more distant craters southeast of the spacecraft have relatively low, inconspicuous rims, although patches of coarse blocks can be seen very close to the horizon on the rim of one of these craters.

About 20 craters, that range in diameter from about 3 to 100 m, have been recognized in the field of view below the horizon. These craters have been observed only under relatively high solar illumination, and more craters of comparable size will probably be recognized at low Sun angles. One of the most prominent of these larger craters (fig. 24), which lies about 11 m from the spacecraft, is about 3 m wide and about 2/3 m in depth. It has a distinct but irregular raised rim and a lumpy appearing inner wall that slopes somewhat less than 28 deg. Most of the other craters in the size range of 3 to 20 m have low, rounded, inconspicuous rims or are rimless. The larger craters, taken together, resemble in distribution and form the craters of equivalent size observed in the Ranger photographs in Mare Cognitum and Mare Tranquillitatis.

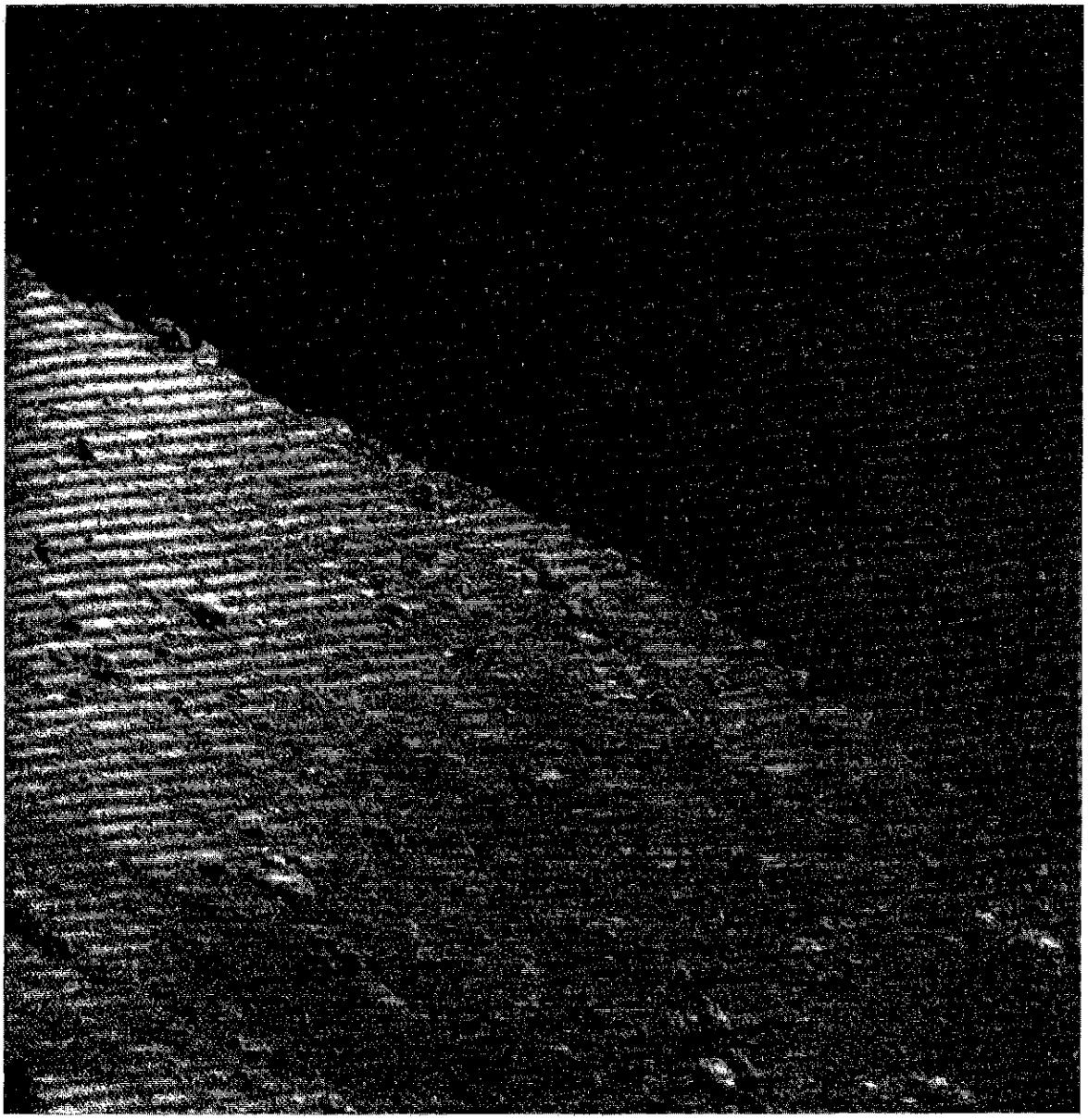

FIGURE 23. — Sector of rim of large crater on horizon, southeast of the spacecraft. Coarser blocks are probably more than a meter in width.

The smaller craters, ranging in diameter from a few centimeters to 3 m, are generally shallow and difficult to observe under high solar illumination. Most of them either have low rounded rims or are apparently rimless. Where they can be observed, close to the spacecraft, they are relatively closely spaced and may cover as much as 50 percent of the surface. More details on their size, shape, and spatial distribution are expected to be obtained from pictures that will be taken in the late lunar afternoon.

Distribution of Blocks and Coarser Debris

The lunar surface in the vicinity of the spacecraft is littered with coarse blocks and fragments. Most of the more prominent blocks in

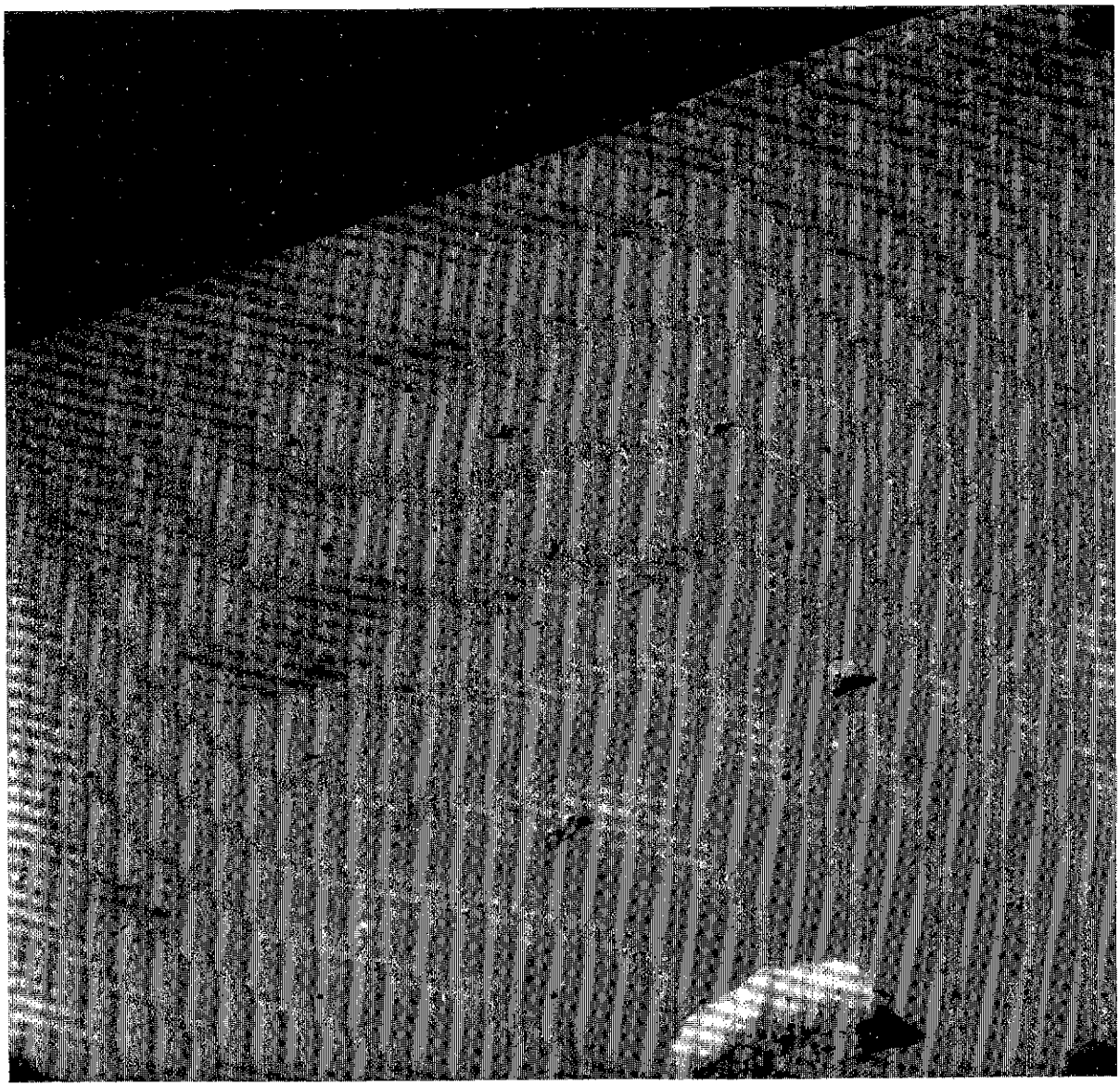

FIGURE 24. — Crater approximately 3 m in diameter, southeast of spacecraft.

the field of view appear to have a nearly random distribution over the surface, but significant concentrations of blocks and finer rubble occur in certain locations. A strewn field of very coarse, relatively closely spaced blocks surrounds the crater noted on the eastern horizon (fig. 23). This field extends from the rim crest of the crater out to a distance of about 1 crater diameter in each direction along the horizon. It is highly probable that the large majority of these blocks are a part of a more or less continuous blanket of ejected debris surrounding the crater and that most of these blocks have been derived from within the crater.

A fairly large number of the blocks observed on the horizon formed by the crest of the crater rim have angular widths as great as 15 min of arc. If the rim of the crater is as much as 300 m or more from the spacecraft, blocks with these angular dimensions must all be more than 1 m

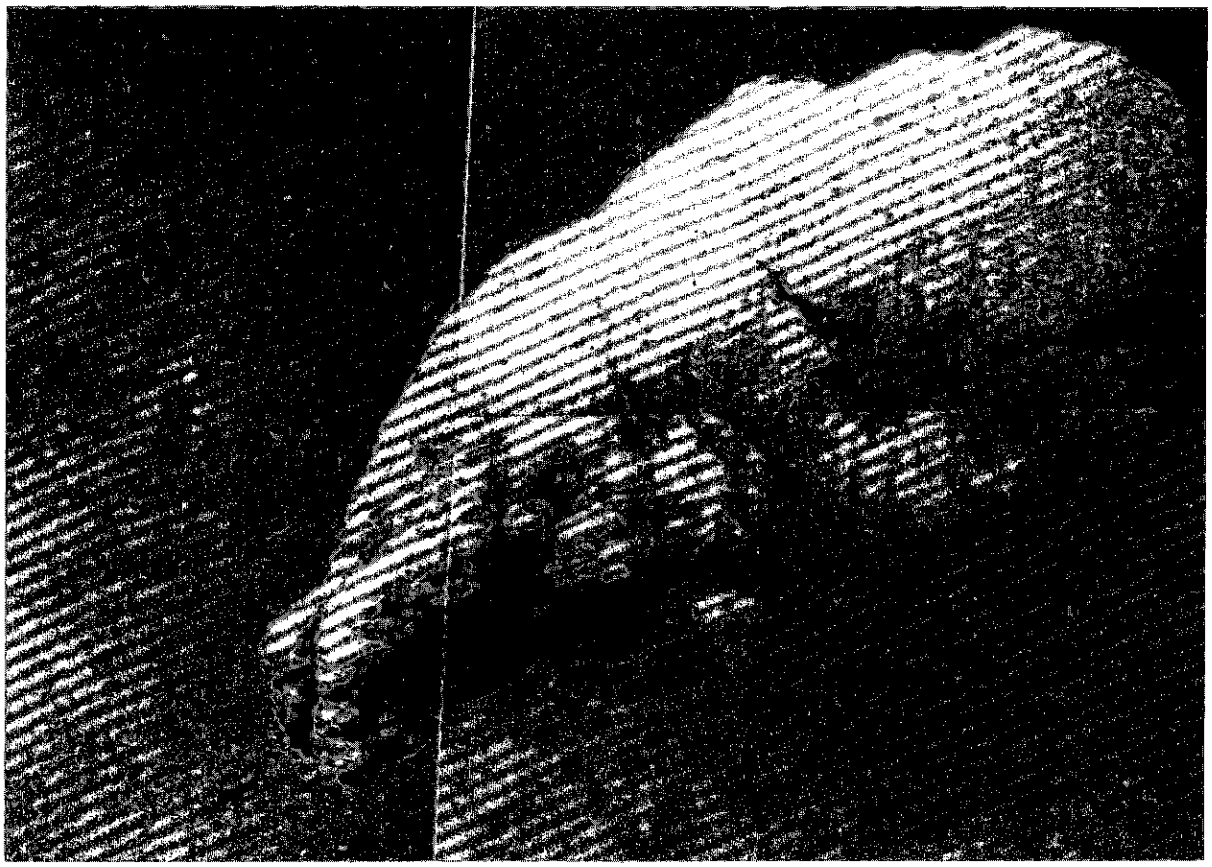

FIGURE 25. — Rock approximately 0.5 m long, southeast of spacecraft. Dark spots are pores or cavities.

across. Other blocks, associated with a still more distant crater rim, are also probably more than 1 m across; some of them have angular widths of more than 20 min of arc.

In the foreground and middle distance are scattered patches of rubble with an average grain size much less than that of the nearby coarser blocks but significantly greater than the average resolvable grain size of nearby parts of the surface. These patches resemble flattened piles of rubble derived from the slow-speed impact of weakly coherent material thrown out of experimental craters produced by explosion and impact on Earth. Some of the patches around Surveyor I occur within the shallow depressions, which may be secondary-impact craters.

Most of the coarser blocks scattered about the surface appear to be equant in shape and are angular to subangular; a small number are subrounded. The majority of the angular blocks appear to rest on the surface, with perhaps 80 to 90 percent of their bulk above the surface level. Many of the round blocks seem to be partially buried; in some cases, perhaps 50 percent or more of the block is below the surface level. None of the fragments or blocks is seen to rest on pedestals, as has been suggested by some Soviet scientists on the basis of the Luna IX photographs.

The angular blocks, especially those on the rim of the prominent crater on the eastern horizon, are typically faceted as though broken along joints and pre-existing fractures. Some of the large blocks along the horizon appear to be resting on top of the surface and have demonstrable overhangs (fig. 23). These blocks must have substantial cohesion and shear strength, particularly if they have arrived in their present

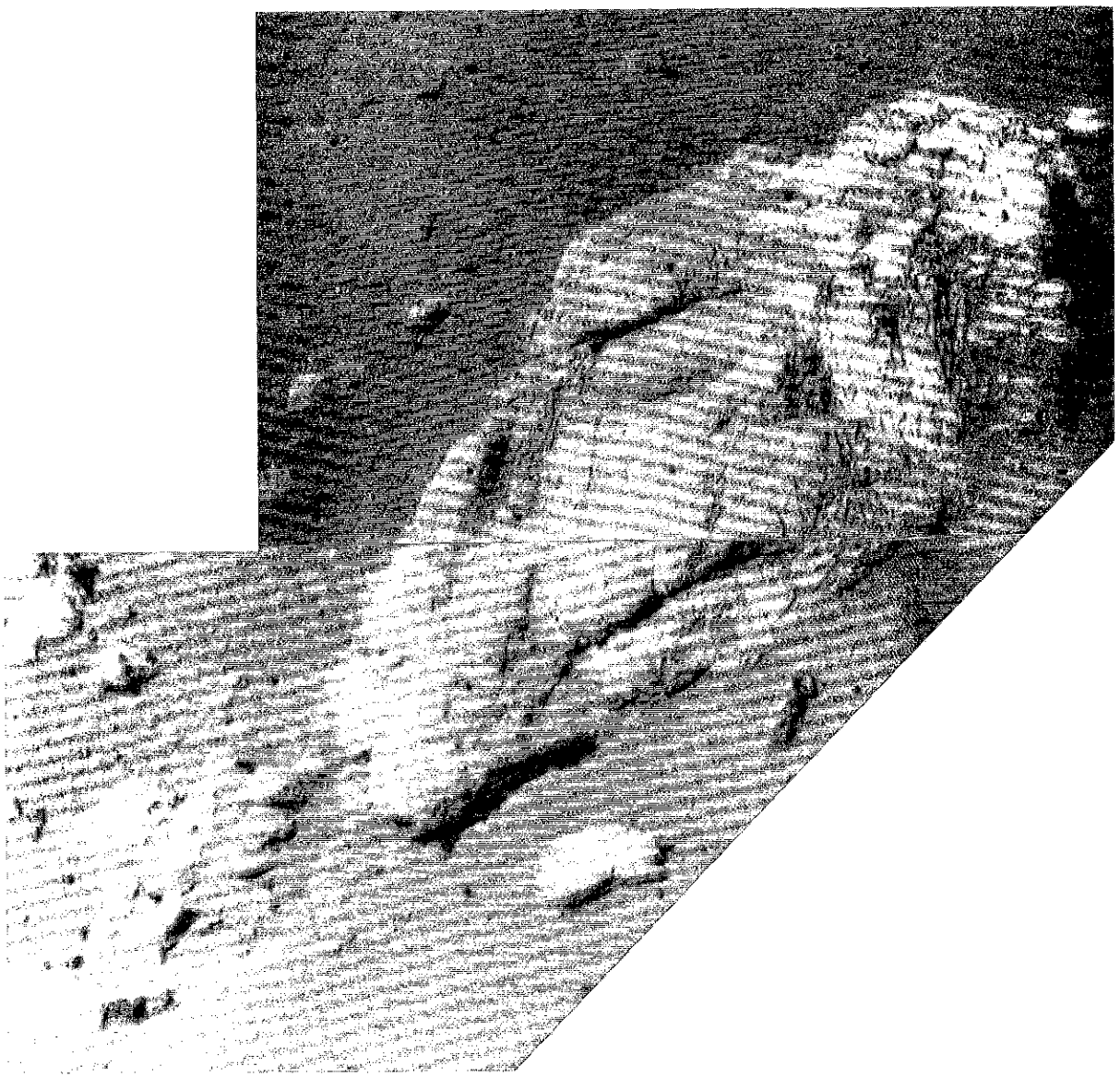

FIGURE 26. – Block with rounded edges and associated fragments, southwest of spacecraft. Note mottling and fractures on main block.

position by ejection from the crater. The very large majority of the coarser blocks have, in addition, a demonstrably higher albedo than most of the rest of the lunar surface in the field of view. This is particularly noticeable under high Sun, when the blocks stand out prominently as bright spots. These data suggest that the blocks are composed of material somewhat different physically from the general finer-grained matrix of the lunar surface and that most of them consist of relatively strong single pieces of rock.

Two blocks relatively close to the spacecraft are of special interest. One of these blocks (fig. 25), about 0.5 m across, lies some 5 m southeast and the other (fig. 26), slightly more than 0.5 m across, about 5 m southwest of the camera. The rock to the southeast is distinctly rounded on its upper side, although it is faceted in places and has overhangs on the side facing the camera. The narrow-angle frames show that the block is

distinctly marked with close-spaced dark spots a few millimeters across. Most of the spots are clearly shadows within pores or cavities in the rock surface. They are so close in size to the resolution limit of the pictures that the character of the cavities cannot be determined with confidence. They may be intergranular pore spaces in a relatively coarse-grained rock, or they may be vesicles. The spots exhibit a distinct elongation and pattern, however, which resembles that produced by flowage and distortion of vesicles in a volcanic rock. It seems quite possible that the block observed is a rock congealed from a gaseous melt. Such a melt could have been produced either by strong shock or by vulcanism, and the rock could be an impactite, a volcanic bomb, or a fragment from the top of a vesicular lava flow.

The second block close to the spacecraft is quite different from the first. It is angular in shape, with well developed facets that are slightly rounded at the corners and at the edges. The block appears to be devoid of resolvable granularity, but it is distinctively mottled. The lighter parts of the block tend to stand out as small knobs. The block has the appearance of being somewhat eroded, and the brighter knobs may stand out as a result of differential erosion. One of the most striking things about this block is a very pronounced set of fractures, which appear to intersect and which resemble the cleavage planes produced during plastic flow of rock under moderately high shock pressure. Another striking feature is that the block lies in a swarm of somewhat similar, smaller fragments, which are strewn out in the direction of elongation of the main block. At least 50 separate pieces are present in the swarm. Many of these fragments and part of the base of the block appear to be partially buried in the lunar surface, but a few fragments seem to rest on the surface. The impression gained is that the main piece has broken up, perhaps on impact with the surface, and that it may have relatively low shear strength. No impact or skid marks are observable around the block area or pieces, however. The swarm of fragments may have been lying on the surface for a considerable period of time and been partially buried by younger, finer debris.

Size Distribution of Debris on the Lunar Surface and the Characteristics of the Fine Matrix

The spacecraft appears to be located in a relatively representative part of the terrain in the field of view, and a first attempt has been made to evaluate the size-frequency distribution of fragments making up the observable lunar surface from a series of narrow-angle pictures of small areas relatively near the spacecraft. The pictures used were taken under comparatively high Sun; therefore, only the more prominent grains are recognizable. It is expected that our first estimates of the size-frequency distribution will be slightly biased toward underestimating the actual average grain size.

Four sample areas (fig. 27), 0.23, 0.90, 3.5, and 50 m^2 in size, were selected on the undisturbed surface, ranging in mean distance from 2.5 to about 20 m from the camera. The areas and grain sizes were estimated by transformation of the pictures to a nominal flat surface defined as being at a base of the spacecraft footpads. All sharply formed fragments and grains that are easily recognizable in the pictures were measured and counted; these amounted to a total of 825, ranging in diameter from 1 mm to more than 1 m.

The integral frequency distribution of the grains, normalized to an area of 100 m^2, for each of the sample areas is shown in figure 27. It can be seen from the figure that the sample areas selected provide overlapping coverage in resolution and that the distribution functions of the grains in each area may be roughly described as segments of one overall distribution function. There is clearly some heterogeneity from one small area to another, as would be expected from examination of the lunar surface within the field of view, but the general size-frequency distribution of fragments on the local lunar surface is probably fairly well estimated by the lower solid line in the figure. This line is the plot of the following equation:

$$N = 3 \times 10^5 \, y^{-1.77}$$

where

N = cumulative number of grains
y = diameter of grains in mm

This function is bounded at an upper size limit

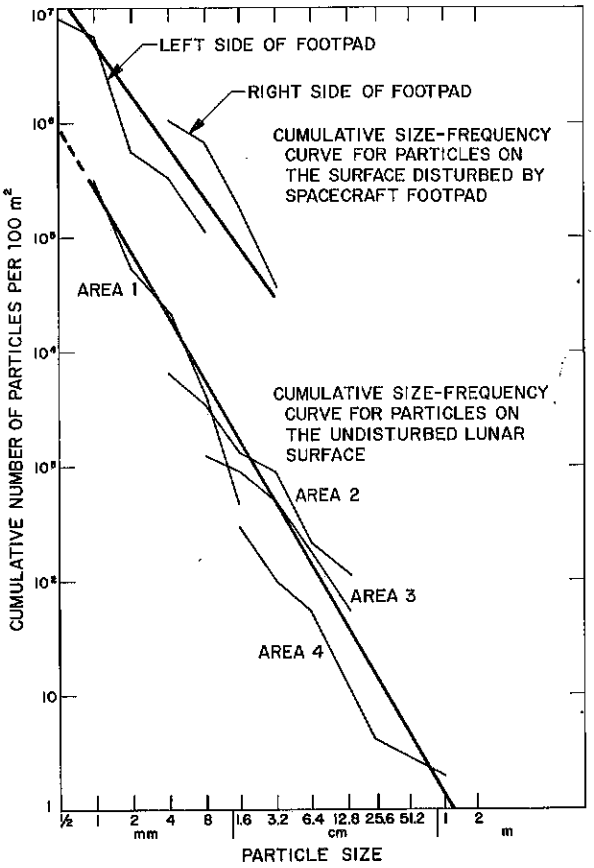

FIGURE 27. — Cumulative frequency distribution of particles on the lunar surface determined from Surveyor I photographs. Area 1 is 0.23 m²; area 2 is 0.90 m²; area 3 is 3.5 m²; area 4 is 50 m² in foreground only.

of about 1 to 2 m but probably extends to particle sizes considerably finer than 1 mm (the limit of the observational data). About one block 1 m across may be expected to be found on each 100 m² of the surface. The mean grain size of the surface material, averaged by particle mass, is probably of the order of about 1 mm. The form and constants of this size distribution function are closely similar to the size-frequency distribution of fragments produced by crushing and grinding of rocks in ball mills and by repetitive impact of rock surfaces.

The matrix of the unresolved material between the grains, where observed very close to the spacecraft, shows a peculiar patchiness of albedo when observed under high Sun. These patches may be caused by successive thin deposits of very fine-grained material derived from different areas.

Material Ejected by Impact of the Spacecraft Footpads

Around footpads 2 and 3 of the spacecraft are ray-like deposits of ejected material extending out in certain directions as far as several tens of centimeters from the edge of each footpad (see fig. 14). These deposits form a distinct raised ridge near each of the footpads. The ejected material differs both in albedo and in texture from the material exposed on the adjacent undisturbed parts of the lunar surface. The average albedo of the ejected material is nearly 30 percent lower than that at the undisturbed surface, as estimated by the methods described in the following section. The material is composed of distinctly coarser lumps or fragments of ejecta than the adjacent undisturbed surface material.

The integral size-frequency distribution of the lumps of the spacecraft footpad ejecta was estimated from two sample areas of about 100 and 50 cm², respectively, on either side of footpad 2. A total of about 250 grains and lumps were counted. The observed size-frequency distributions are shown in figure 27, and it can be seen that the footpad ejecta are about an order of magnitude coarser than the material of the surrounding lunar surface. These data strongly suggest that the observed lumps in the freshly ejected material are probably aggregates of much finer grains. The size distribution of the finer grains composing the aggregates is probably given by the mean size distribution function for the general surrounding surface. In all likelihood, the lumps are only weakly consolidated and could be disaggregated into their constituent grains under a modest pressure or agitation. Similar lumps that may be formed around natural impact craters are probably quickly broken down by the ballistic rain of small particles on the lunar surface.

Photometry and Colorimetry

One of the important functions of the television camera is its use as a photometer. For the first time, the observable photometric function

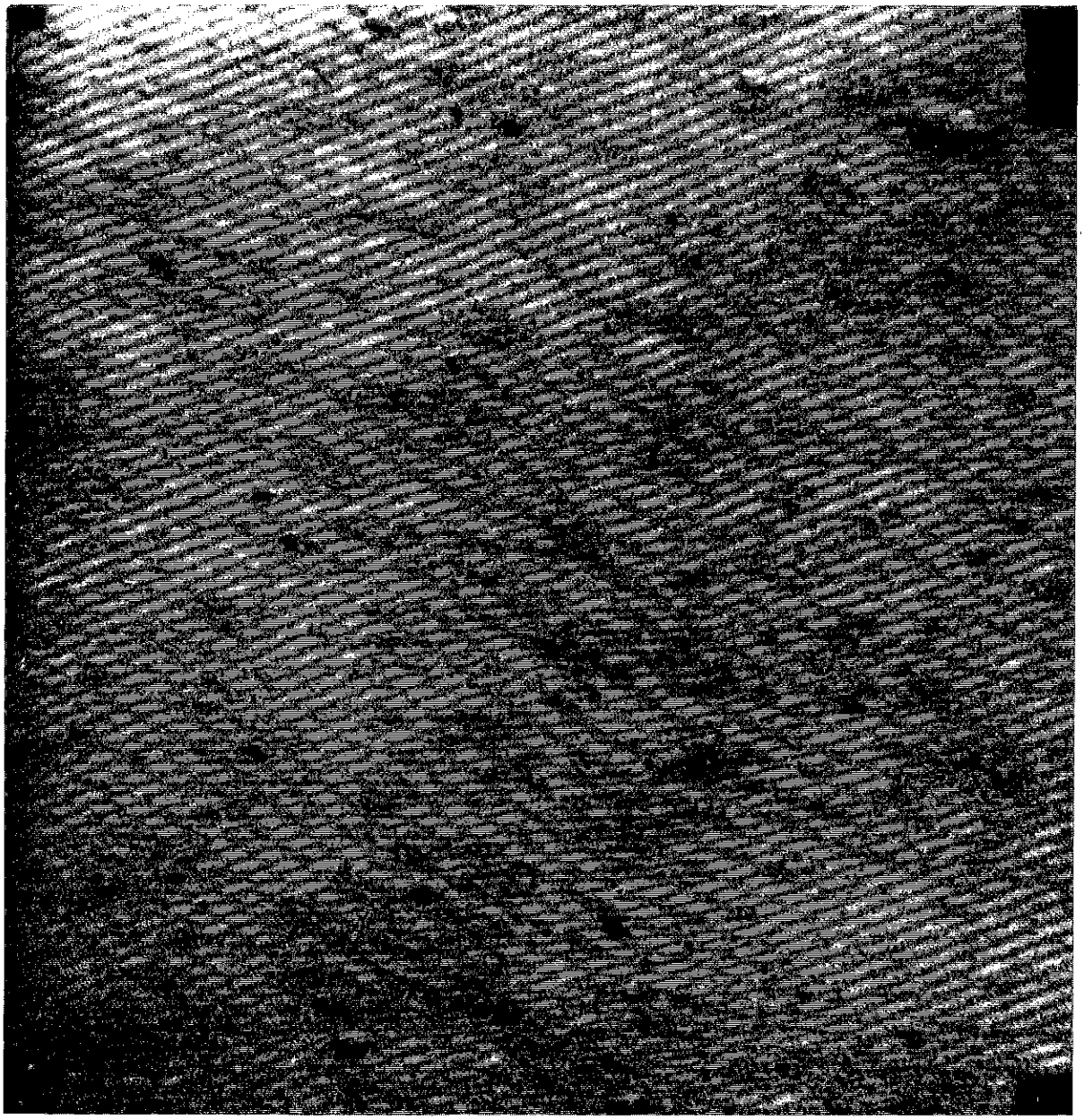

FIGURE 27, Continued. Area 1.

of part of the lunar surface can now be compared with the megascopic texture of the surface. Furthermore, a much more complete measure of the function can be obtained at one lunar location than from Earth-based observation, and it will be possible to test in detail the assumed symmetry or degeneracy of the photometric function.

The location of the landing site near the lunar equator enabled measurements of the surface luminance to be made almost every day in the plane of the Sun-slope normal. The measurements were calibrated by photographing the photometric target before and after each survey. The stability of the camera between these measurements was about 10 percent. Three frames of

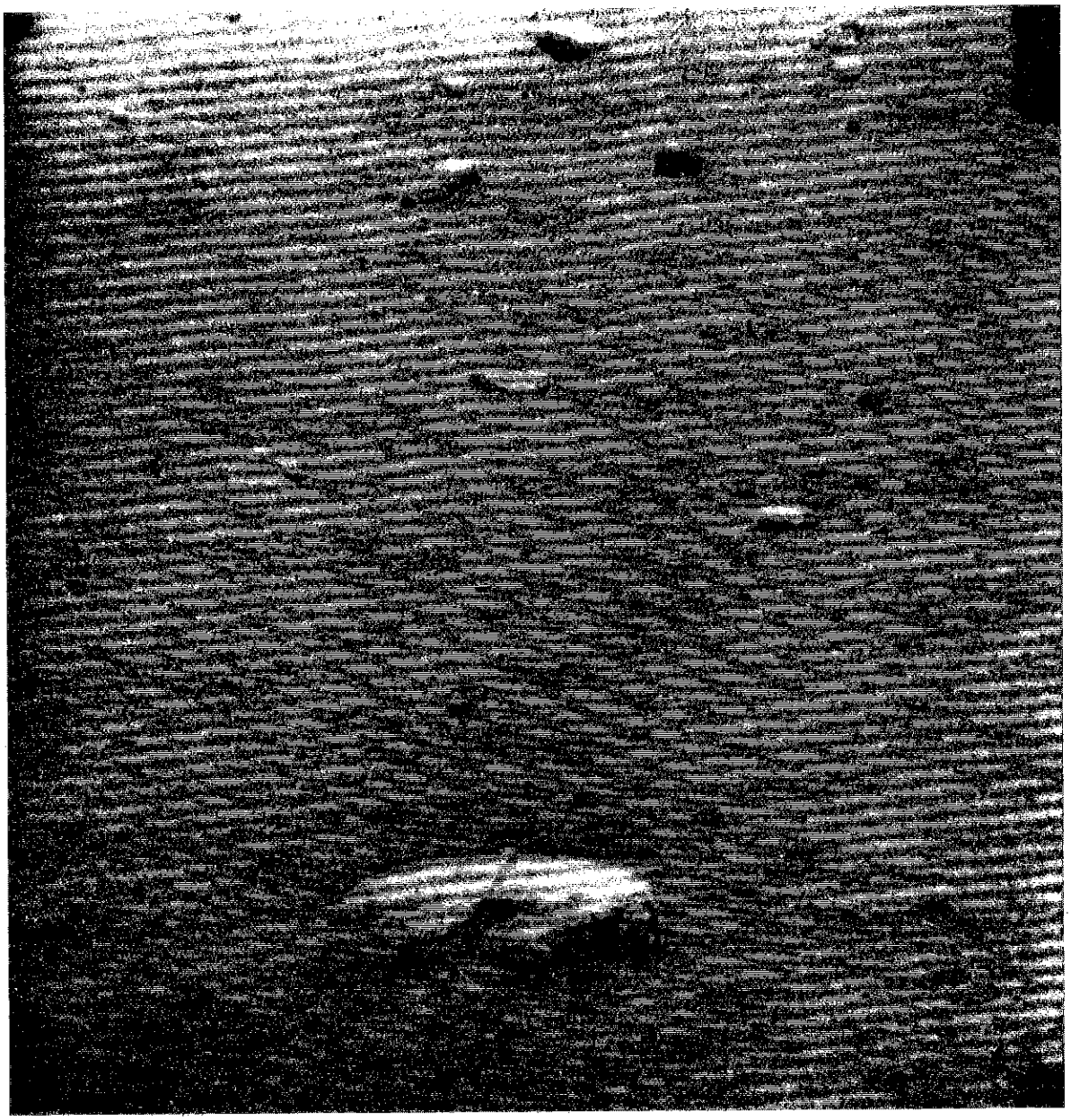

FIGURE 27, Continued. Area 2.

the photometric target were selected for repeatability checks. The variation between these sequential frames was approximately 2 percent.

The photometric target was calibrated before flight by a goniophotometer, and its orientation on the spacecraft made normal to the camera's center line of sight. The calibration data have been used in conjunction with the photometric angles of phase, incidence, and emergence to predict luminance values for each target step.

The video signal has been recorded on magnetic tape and by a flying spot scanner photo recorder. Control of the processing of the film has indicated that a high degree of stability exists between the film records. A transfer characteristic from such a negative to the photometric

FIGURE 27, Continued. Area 3.

target is shown in figure 28. The latitude of the film (SO-337) is great enough so that the entire video transfer characteristic may be recorded on the linear portion of the film.

As a preliminary check on the use of the camera as a photometer, the scene luminance was measured for parts of the lunar surface surrounding the pad upon which the photometric target was mounted. By fitting the measured scene luminance to the photometric function derived from the telescopic measurements of Fedorets (ref. 5), an estimate of 7.7 percent for the normal albedo was derived for the parts of the surface which appeared to be undisturbed by the pad (fig. 14). The estimated albedo for the disturbed areas was about 2 percent lower.

FIGURE 27, Continued. Area 4.

In general, the terrain exhibits the gross luminance values expected from the telescopically determined average of the photometric function of the maria. As further data are obtained in the lunar afternoon, the local normal albedo can be determined more precisely.

The light scattered from the spacecraft is a particular problem in evaluating the luminance of the lunar surface. Areas in the immediate spacecraft vicinity (2 m) are partly illuminated by light scattered from the spacecraft, especially at low Sun angles. The contribution of light from the spacecraft fills in the shadows to such a degree that an additional photometric target mounted on the B omniantenna was clearly discernible with the chart averted from the Sun.

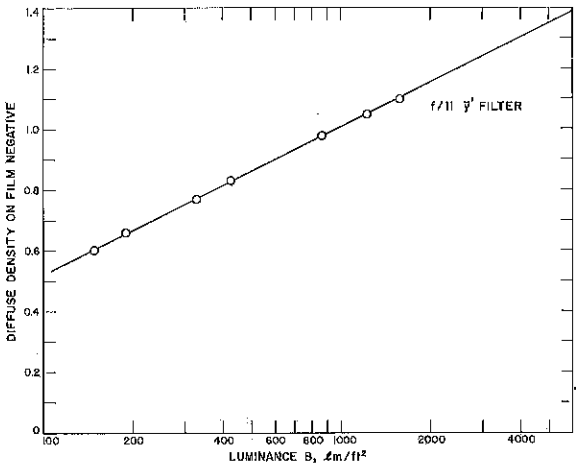

FIGURE 28. — Total television system transfer characteristic function determined from observation of the photometric target on the spacecraft leg during lunar operation.

Several color surveys using the three filters were made, beginning the third day after touchdown. The main purpose of these surveys was to ascertain whether or not there are color differences in the vicinity of the spacecraft. The data so obtained permit estimates to be made of the spectral reflectances. Again, to check and maintain the calibration of the camera-filter combination, the photometric target was observed with each filter before and after the survey (fig. 20). Preliminary examination of the prominent mottled rock lying just southwest of the spacecraft (fig. 26) indicates that any color differences that may be present in the surface of the rock are very small. Much more careful processing of the video data is necessary before subtle color differences can be measured.

Lunar Surface Electrical Properties

FIVE DAYS AFTER THE TOUCHDOWN of Surveyor I, the radar signal-strength data were still under detailed analysis to determine the average radar cross section in the vicinity of the landing site. The radar frequencies used by the spacecraft were 9 300, 12 900, and 13 300 Mc. If it proves possible to deduce the effective reflectivity, effort will be made to calculate some of the electrical characteristics of the lunar surface. No tentative conclusions, however, are as yet warranted at the time of this writing.

REFERENCES

1. SHORTHILL, R. W., AND SAARI, J. M., *Isotherms in the Equatorial Region of the Totally Eclipsed Moon:* Boeing Geo-Astrophysics Laboratory, Report DI-82-0530, Seattle, Washington, April 1966.
2. WECHSLER, A. E., AND GLASER, P. E., "Thermal Properties of Postulated Lunar Surface Materials," *The Lunar Surface Layer,* Salisbury, J. W., and Glaser, P. E., Editors, New York and London, Academic Press, 1964, pp. 389-410.
3. JAFFE, L. D., "Mechanical and Thermal Measurements on Simulated Lunar Surface Materials," *The Lunar Surface Layer,* Salisbury, J. W., and Glaser, P. E., Editors, New York and London, Academic Press, 1964, pp. 355-380.
4. H. KNUDSEN of Hughes Aircraft Company suggested working from the outer canister temperature on Compartments A and B to establish lunar surface temperatures. M. GRAM of JPL carried out the premliminary thermal analysis.
5. FEDORETS, V. A., "Photographic Photometry of the Lunar Surface," *Reports of the Astronomical Observatory of the Charkow State University,* Vol. 2, 1952.

APPENDIX A

Membership of Surveyor Scientific Evaluation and Analysis Team

To meet program scientific objectives, the Surveyor Scientific Evaluation and Analysis Team was established to provide a means to study the scientific data produced. In addition to the main Analysis Team, four associated working groups (Lunar Surface Mechanical Properties, Thermal Properties, Topology and Geology, and Electrical Properties) were formed to investigate in detail various aspects of the data. Analysis Team members include the Investigators on later Surveyor missions, the Jet Propulsion Laboratory Surveyor Project Scientist, and the National Aeronautics and Space Administration Surveyor Program Scientist. Members of these groups who contributed to the respective sections of this article are:

Surveyor Scientific Evaluation and Analysis Team

L. D. JAFFE, *Chairman*	Jet Propulsion Laboratory
S. E. DWORNIK	NASA Headquarters
W. M. ALEXANDER	Temple University
S. A. BATTERSON	Langley Research Center
R. F. SCOTT	California Institute of Technology
E. M. SHOEMAKER	U.S. Geological Survey
G. H. SUTTON	Columbia University
A. TURKEVICH	University of Chicago

Membership of Working Groups

Lunar Surface Mechanical Properties

S. A. BATTERSON	Langley Research Center
H. E. BENSON	Manned Spacecraft Center
C. E. CHANDLER	Jet Propulsion Laboratory
E. M. CHRISTENSEN, *Chairman*	Jet Propulsion Laboratory
R. H. JONES	Hughes Aircraft Company
R. F. SCOTT	California Institute of Technology
E. N. SHIPLEY	Bellcomm, Inc.
F. B. SPERLING	Jet Propulsion Laboratory
G. H. SUTTON	Columbia University

Lunar Surface Thermal Properties

J. E. CONEL	Jet Propulsion Laboratory
R. B. ERB	Manned Spacecraft Center
R. R. GARIPAY	Hughes Aircraft Company
W. A. HAGEMEYER	Jet Propulsion Laboratory
J. W. LUCAS, *Chairman*	Jet Propulsion Laboratory
J. M. SAARI	Boeing Science Laboratory

Lunar Surface Topography and Geology

E. M. SHOEMAKER	U.S. Geological Survey
W. M. ALEXANDER	Temple University
J. L. DRAGG	Manned Spacecraft Center
E. C. MORRIS	U.S. Geological Survey
J. J. RENNILSON, *Acting Chairman*	Jet Propulsion Laboratory
A. TURKEVICH	University of Chicago

Lunar Surface Electrical Properties

W. E. BROWN, JR., *Chairman*	Jet Propulsion Laboratory
R. A. DIBOS	Hughes Aircraft Company
D. O. MUHLEMAN	Cornell University

APPENDIX B

Surveyor Management Team

National Aeronautics and Space Administration

H. E. NEWELL	Associate Administrator for Space Science and Applications
E. M. CORTRIGHT	Deputy Associate Administrator for Space Science and Applications
R. F. GARBARINI	Deputy Associate Administrator for Space Science and Applications (Engineering)
O. W. NICKS	Director, Lunar and Planetary Programs
B. MILWITZKY	Surveyor Program Manager
W. JAKOBOWSKI	Surveyor Program Engineer
F. A. ZIHLMAN	Surveyor Program Engineer
S. E. DWORNIK	Surveyor Program Scientist

Jet Propulsion Laboratory

W. H. PICKERING	Director
A. R. LUEDECKE	Deputy Director
R. J. PARKS	Surveyor Project Manager
H. H. HAGLUND	Deputy Project Manager
W. E. GIBERSON	Deputy Project Manager
T. F. GAUTSCHI	Mission Operations System Manager
L. D. JAFFE	Surveyor Project Scientist
N. A. RENZETTI	Tracking and Data System Manager

Hughes Aircraft Company

J. H. RICHARDSON	Senior Vice President
F. ADLER	Vice President and Manager, Space Systems Division
R. L. RODERICK	Surveyor Program Manager
R. E. SEARS	Associate Manager
R. R. GUNTER	Assistant Manager, Test and Operations
F. G. MILLER	Assistant Manager, Engineering and Manufacturing
S. C. SHALLON	Chief Scientist

NASA-Langley, 1966